MARINE
TECHNICAL
REPORT
NUMBER 97-1

The August 93 North Edisto Ingress Experiment (NED2)

J. Blanton
J. Amft
P. Verity
C. Barans
E. Wenner

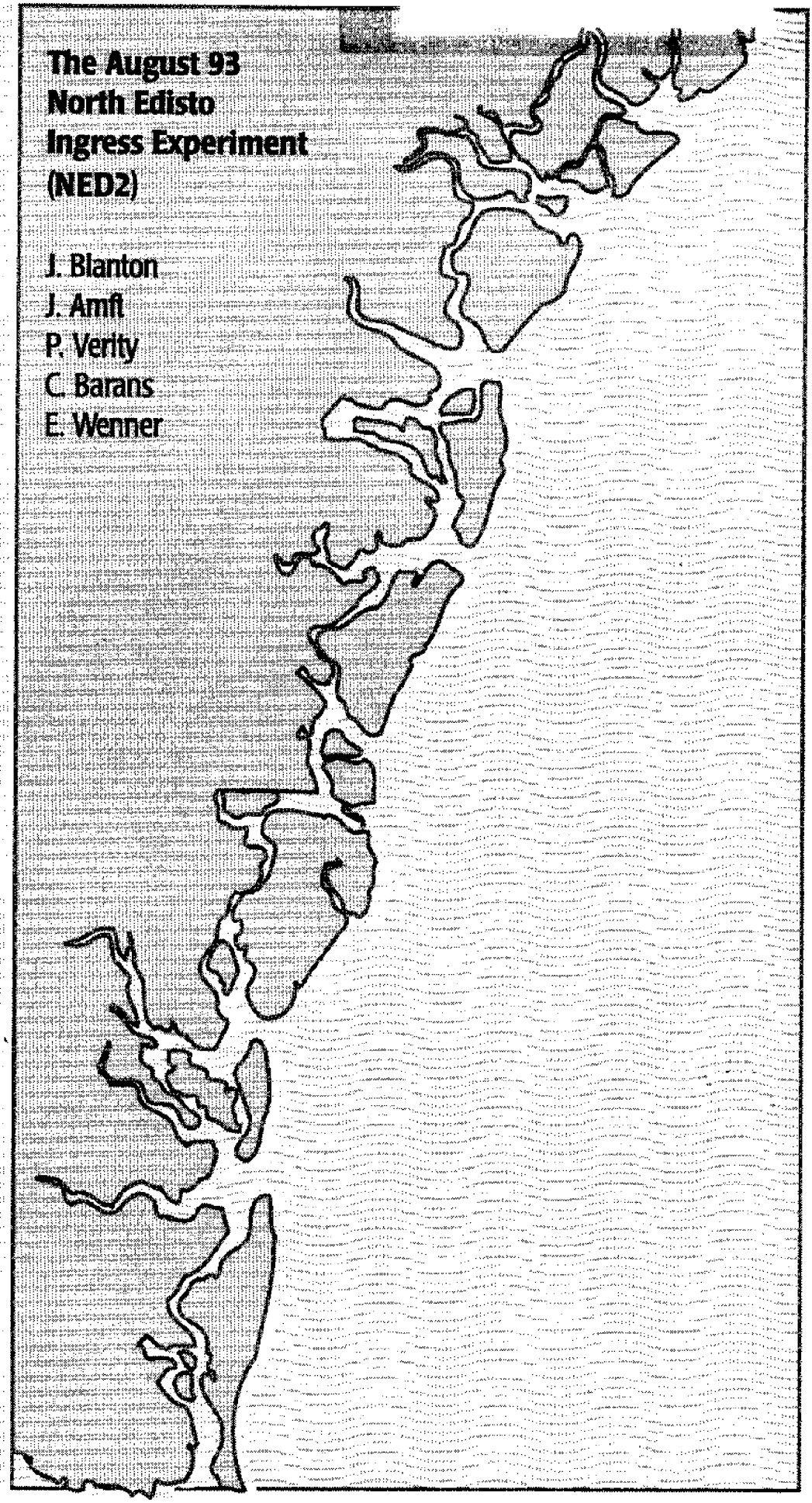

The University of Georgia

School of Marine Programs
Athens, Georgia

The August 93 North Edisto Ingress Experiment (NED2)

Technical Report

J. Blanton, J. Amft, P. Verity

Skidaway Institute of Oceanography
10 Ocean Science Circle
Savannah, Georgia 31411

C. Barans and E. Wenner

South Carolina Marine Resource Research Institute
P.O. Box 12559
217 Ft. Johnson Road
Charleston, SC 29422-2559

The Technical Report Series of the Georgia Marine Science Center is issued by the Georgia Sea Grant College Program and the Marine Extension Service of the University of Georgia on Skidaway Island (30 Ocean Science Circle, Savannah, Georgia 31411). It was established to provide dissemination of technical information and progress reports resulting from marine studies and investigations mainly by staff and faculty of the University System of Georgia. In addition, it is intended for the presentation of techniques and methods, reduced data, and general information of interest to industry, local, regional, and state governments and the public. Information contained in these reports is in the public domain. If this pre-publication copy is cited, it should be cited as an unpublished manuscript. This work was sponsored by joint grants from the Georgia Sea Grant Program (Grant No. R/EA-15) to the Skidaway Institute of Oceanography and the South Carolina Sea Grant Consortium (Grant No. 93277) to the South Carolina Marine Resource Research Institute.

ACKNOWLEDGMENTS

We wish to express our appreciation to the several individuals without whose help this project would not have been possible. First, our thanks go to Marsha Ward who participated in the cruises and Lane Mitcham of Skidaway Institute who developed much of the instrumentation and software used in the ODIS system aboard the BLUE FIN. Next, we thank Bruce Stender and David Knott of the South Carolina Marine Resources Research Institute, our scientific partners in this project. We also appreciate the able support of Captain Jay Fripp and crew Chris Knight and Billy Harrell of the R/V BLUE FIN, and Captain Paul Tucker of the R/V ANITA.

This work was sponsored by joint grants from the Georgia Sea Grant Program (Grant No. R/EA-15) to the Skidaway Institute of Oceanography and the South Carolina Sea Grant Consortium (Grant No. 93277) to the SC Marine Resource Research Institute.

ABSTRACT

A 14-day field experiment was conducted between 25 August and 7 September (NED2). The experiment was designed to determine the oceanographic factors important to the ingress of postlarval *Penaeid* and megalopae of *Callinectes sapidus* through the North Edisto Inlet, South Carolina. Two distinct wind regimes occurred during this 14-day field experiment. The first five days were calm, and coastal waters were weakly stratified to well-mixed. Winds during the following six days were favorable for upwelling, and coastal currents flowed northeastward. Maximum vertical stratification was observed on the ocean side of the inlet's delta during calm winds of the first five days. The water column here became well-mixed during increased wind stress of the upwelling wind regime. Weak stratification reappeared as the upwelling wind regime relaxed during the final three days. Strong horizontal salinity gradients between the inlet and open continental shelf suggested that communication between ocean and inlet was inhibited to some degree.

Results from NED2 and its predecessor, NED1, revealed the importance of onshore wind stress. The most efficient stress for Penaeid postlarvae was downwelling winds with an onshore component. Ingress of megalopae occurred when wind was favorable for upwelling, particularly when there was an onshore wind stress component.

Horizontal gradients of chl *a* were dominant on the continental shelf, while vertical gradients (increasing concentration with depth) were prominent near the delta separating the ocean from the inlet. This suggests that the delta region was a benthic source of phytoplankton to shelf waters. Thus the ocean-estuary interface may act as a food source for the larvae entering the estuary.

Keywords: Shrimp, Coastal, Estuaries, Fisheries, South Carolina, Hydrodynamics, Hydrography, Inlet, Larvae, Meteorology, Oceanography, Plankton, Recruitment, Upwelling, Downwelling, Fronts

LIST OF TABLES

LIST OF FIGURES

Table of Contents

The August 93 North Edisto Ingress Experiment (NED2)

by

J. Blanton, J. Amft, P. Verity, C. Barans and E. Wenner

1.0 Purpose and Objectives

This report summarizes data and results from NED2, the August-September 1993 North Edisto Ingress Experiment. This is the second of a series of cruises designed to relate the spatial and temporal distribution of postlarval blue crab and white shrimp in inner shelf water entrained through an inlet to periodic (tidal, diel, lunar) and stochastic (wind, current) events.

As was its predecessor, NED1 (Blanton et al. 1994a), NED2 was designed to determine: (1) the hydrography of the coastal frontal zone adjacent to a study site and corresponding abundances of larvae or megalopae; (2) the hydrographic state of the inlet water and corresponding abundances of larvae or megalopae; and (3) the response of shelf and inlet waters to wind and tides.

NED2 was conducted in and off the North Edisto Inlet on the South Carolina coast (Fig. 1a) in late summer (August-September) 1993. This time period precedes the autumn season when prevailing winds normally favor downwelling, and the coastal frontal zone is vertically well mixed. Freshwater discharge to the coast is seasonally low. Blue crab megalopae usually are present in coastal waters at this time. The sampling period covered 14 days. Because the tidal cycle is 12.48 hrs (2 cycles in 24.96 hrs) and the diurnal cycle is 24 hrs, a sampling of the same tidal stage over the 14-day period covers a full cycle of spring-neap tides and half-cycle of sunlight.

2.0 Oceanographic Methods Used

We utilized a combination of moored instrumentation and shipboard sampling. One mooring was positioned on the inner continental shelf to assess the response of the alongshelf current to wind forcing. Another mooring was deployed in the deep inlet channel with a TRACOR ACOUSTIC PROFILING SYSTEM (Holliday 1992) to monitor the acoustic return signal together with currents, salinity and subsurface pressure.

As in NED1, the mooring data were complemented by frequent hydrographic and larval abundance surveys both in the inlet and offshore. Thus, the combined synthesis of *in situ* data and shipboard data provided us the means to determine: (1) the temporal variations in coastal water advected into the inlet; (2) the location of larval populations relative to the coastal front; and (3) temporal variations in larval abundance advected into the inlet during flood tide.

2.1 Moored instruments

Oceanographic information was collected from two moored instrument arrays, designated as 'M1' and 'M2' (Fig. 1a), for approximately two weeks in August-September 1993. M1 was placed nearshore north of the main channel of the North Edisto River in water 17.5 meters deep (the main channel is 21 meters deep). M2 was located about 10 nautical miles (18 km) offshore approximately at the 14-meter isobath.

Two InterOcean Systems, Inc. S4 current meters and two Sea-Bird Electronics, Inc. SEACAT data loggers were deployed at each site to measure currents, temperature and conductivity at two levels in the vertical and subsurface pressure at the bottom (Fig. 2; Table 1). Salinity and density (σ_t) were derived from conductivity, temperature and pressure values. The sampling rate for all the moored instruments was six minutes (0.1 hour).

Wind speed and direction, barometric pressure, and air temperature were monitored hourly at Folly Beach (FBIS1), a nearby C-MAN (Coastal-Marine Automated Network) station which is

maintained by the National Oceanic and Atmospheric Administration (NOAA). FBIS1 is about 30 kilometers east-northeast of the North Edisto River study area. The meteorological information obtained at this station should represent local conditions. The wind speed and direction files were converted to x and y components. The corresponding surface wind stress components were calculated by an iterative technique (Blanton et al. 1989b), which adjusted the wind speed to a 10-meter level and used a variable drag coefficient depending on the magnitude of the wind speed.

2.2 Shipboard sampling

Seven hydrographic and larval abundance surveys were conducted offshore aboard the R/V BLUE FIN of the Skidaway Institute of Oceanography. For NED2 the R/V ANITA, of the South Carolina Marine Resources Research Institute, conducted eight surveys in the inlet throat; the R/V BLUE FIN carried out the first throat survey.

The BLUE FIN generally occupied offshore stations on the adjacent continental shelf (Fig. 1a) in an attempt to map the structure of the coastal frontal zone and the distribution of larval abundance perpendicular to shore. Transects alternated along the N-line and the S-line of stations in order to determine whether systematic differences occurred north or south of the delta. The timing of the offshore surveys was set to reach either station N1 or S1 at the maximum flood tide which best coincided with the nighttime surveys in the throat. The "A" stations (Fig. 1a) demarcate the seaward extent of the ebb tide data, and A6 was sampled regularly in the offshore surveys.

The ANITA was stationed in the North Edisto throat and sampled during nighttime flood tides at three positions across the throat designated "N" (north), "M" (middle) and "S" (south). These station locations are depicted as three short parallel lines near mooring M1 on Figure 1b. The throat surveys were designed to measure oceanographic properties of temperature, salinity, density and larval abundance entering the inlet and ascertain lateral variability in these parameters.

2.2.1 Hydrographic sampling

Each ship recorded vertical profiles of conductivity (C), temperature (T), fluorescence (Fl) and depth (D) using a Sea-Bird Electronics, Inc. Model 25 Sealogger CTD. Salinity and density were calculated from the conductivity, temperature and depth values using standard algorithms. An optional fluorometer was installed on each unit, and the CTD on the BLUE FIN also had an optical backscatter (OBS) sensor. The fluorometer was designed to measure chlorophyll *a* fluorescence (Fl) and the OBS sensor measured turbidity by detecting infrared radiation scattered from suspended matter. The OBS values were not calibrated with suspended sediment samples, so they represent relative turbidity only. Detailed information on CTD sensor specifications, sampling protocol and data processing procedures are covered in Blanton et al. 1994a.

The CTD was set up to sample all the above parameters (C, T, D, Fl, OBS and calculated salinity and density) at 1 Hz in real-time mode. Thus, the vertical structure of the water column could be ascertained immediately. The CTD cast information also was stored as a binary data file (with a sample rate of 4 Hz). Software provided by Sea-Bird Electronics allowed several ways to view the data, including graphical or tabular display of the variables.

As part of the post-deployment processing, data from each CTD downcast were averaged by depth into 1.0 meter bins. The bin-averaged data then were grouped appropriately to create contour plots of selected parameters, such as temperature, salinity and fluorescence.

The station logs (Tables 2 and 3) indicate the timing and position for the 91 CTD casts taken on the BLUE FIN and the 53 casts from the ANITA. A more graphical representation shows the relative schedules for the various offshore and throat surveys for each vessel (Fig. 3).

The throat and offshore surveys were intended to sample the inlet and nearshore regions as contemporaneously as possible. However, since the nighttime flood tide was about one hour later every day (2 semi-diurnal tidal cycles – 25 hours), the offshore surveys gradually progressed out of the

nighttime hours, and many offshore stations were sampled during the day. The original schedule also was interrupted by the threat of a hurricane. Additionally, we experienced mechanical problems with the ANITA for several days near the beginning of the study period and one throat survey was conducted on the BLUE FIN.

Two surveys, labeled "LW" and "HW" (Fig. 3), represent hydrographic sampling only (no larval sampling) along offshore and estuarine transects centered in time at consecutive low-water and high-water periods. These surveys were designed to show how far water masses were translated during one-half of a semi-diurnal tidal cycle and to see if conditions changed during the neap-to-spring tidal cycle. These surveys will be described in a later section.

2.2.2 Continuous mapping of near-surface ocean properties

An Oceanographic Data Interface System (ODIS) aboard the BLUE FIN was designed to interface with an assortment of instruments. A primary navigation interface consisted of a Global Positioning System (GPS) and a fathometer. Near-surface ocean water was pumped continuously through a suite of sensors interfaced to ODIS that included temperature, conductivity, and fluorescence sensors. The fluorescence output of a Turner Designs fluorometer was calibrated by periodically collecting subsamples exiting the fluorometer and measuring their chlorophyll *a* (chl *a*) content in the lab. ODIS data were logged automatically onto disk during most of the BLUE FIN cruises at sampling intervals ranging from 1 - 2 minutes.

2.2.3 Phytoplankton biomass sampling

Vertical profiles of fluorescence representing phytoplankton biomass were measured aboard each ship. The Sea-Bird CTDs used aboard the BLUE FIN and ANITA were equipped with SEA TECH *in situ* fluorometers. Prior to the cruises, both were calibrated against the same phytoplankton cultures. These tests showed that the fluorescence output of both instruments was linear over their maximum

range. During the cruises, natural plankton samples were collected at the surface by bucket immediately adjacent to the CTD during selected vertical profiles. Subsamples were concentrated on filters, extracted later in acetone, and chl *a* was measured in the lab using a Turner Designs Fluorometer. These data were used to derive calibration curves to convert *in situ* fluorescence from CTD vertical profiles into chl *a* (Fig. 4).

2.2.4 Larval sampling

Twenty-seven net tows in the offshore domain were taken at stations outside the coastal front, inside the coastal front and at A6 along the arc; A6 was sampled near the time of maximum flood current. Twenty-four tows in the inlet were done in the North Edisto throat (near M1; see Fig. 1b) and sampled during nighttime flood tide at three positions across the throat designated "N" (north), "M" (middle) and "S" (south). This plan complements the hydrographic sampling plan in the inlet described at the beginning of Section 2.2. Inboard and outboard nets were set at surface and bottom at each station using 0.6m bongo nets (0.505 mesh) fitted with an opening and closing device. Tow duration was approximately 5 minutes in the throat and 10 minutes offshore.

3.0 Results and Discussion

Results from NED2 are described by a series of tables and plots that come from moored and shipboard instrumentation. The main forces that affect estuarine and coastal waters are bottom friction induced by tidal and wind-generated currents, barotropic pressure gradients associated with set-up or set-down of coastal sea level, baroclinic pressure gradients caused by horizontal density differences and surface wind stress. These forces not only govern the strength and direction of currents, but also affect the degree of stratification imposed by buoyancy sources from freshwater discharges along the coast and surface heating. The role of these interacting forces will become obvious in the discussion of results that follow.

3.1 Wind stress events

The alongshelf component of wind stress is the principal driving force for coastal currents and wind-driven sea level fluctuations. However, as we found out in NED1, the cross-shelf component also can induce significant transport through the inlet. Figure 5 shows the rotated component and vector plots of wind stress that have been subjected to a 40-hour low-pass filter. (Filtered data sets are discussed in the next section.)

The wind stress record can be divided into three distinct regimes (Fig. 5). Wind stress during the first five days was weak (< 0.03 Pa). An onshore component was present throughout the period, but the alongshore component diminished to nearly zero after the first day of this period. On 31 August, after a hurricane passed about 100km seaward, the second regime began and lasted another six days. This regime, consistently stronger than the first one, was made up of upwelling favorable winds with an onshore component. The third regime consisted of calm winds that lasted only one day before the field experiment ended.

Blanton et al. (1989a, 1994b and 1995) discussed the significance of upwelling and downwelling near-surface regimes on the coastal frontal zone. The essential point for shallow coastal waters such as these is that wind-generated near-surface transport, while to the right of the wind vector in waters where surface and bottom boundary layers are clearly separated, goes essentially downwind in shallow water where these two boundary layers merge. It is here that the cross-shelf wind component reaches an importance that may equal the along-shelf component associated with upwelling and downwelling. The significance of the wind regimes for NED2 will be evident in the offshore transect contour plots of temperature, salinity, density and chlorophyll *a* described in a later section.

3.2 Moored instrument statistics

All moored instruments at M1 and M2 had a 6-minute sample rate, but for this analysis every tenth value was selected to create hourly records. Then, the hourly values for both the oceanographic

and meteorological data were filtered independently with a 3-hour and 40-hour low-pass digital filter. The 3-hour filter (3hlp) removes the high frequency noise from the record, and the 40-hour filter (40hlp) removes variations associated with phenomena which have periodicities of less than 40 hours (i.e., mainly tides). The 3hlp values have a delta-t of 1 hour, while the 40hlp files have been subsampled to a delta-t of 6 hours.

The coordinate system for all current and wind stress vectors was rotated 50 degrees clockwise, so the y axis would closely parallel the local shoreline and isobaths. For this rotated coordinate system, positive x components are directed offshore and positive y components are alongshore toward the northeast.

Three tables of statistics present first order properties for the filtered data sets (Tables 4, 5 and 6). Table 4 shows 3hlp and 40hlp statistics for the complete data sets. The effect of the low-pass filter is most evident in the currents where the 40hlp standard deviations are significantly smaller than the corresponding 3hlp values. Reductions in the other ocean parameters are not so large. Hourly wind data are least affected by the filters.

Note that under the coordinate system rotations used, 3hlp currents (which contain most of their variance in the semi-diurnal tide) fluctuate greatest along the axis of the inlet and perpendicular to the shoreline (the x axis). When the tidal variances are excluded by the 40hlp filter, most of the variance in the inlet is still along the x axis (the inlet's axis), while that of the coastal currents offshore is more shore-parallel.

Statistics during neap and spring tide periods illustrate the effects of the larger spring tides on tidal currents (Table 5). The x axis tidal currents increased by 20 and 22 percent in the inlet throat at mid-water and bottom, respectively. Similar increases of 17 and 10 percent were measured in the coastal waters offshore. Subsurface pressure fluctuations (which represent tidal height elevations) were 10%/11% higher at M2/M1 during spring tides compared to neap tides. The amplification of currents

and sea level by spring relative to neap tides generally was less during NED2 than during NED1 (Blanton et al. 1994).

The calm and upwelling wind regimes identified in Section 3.1 were compared (Table 6). During the calm period (Table 6a), currents offshore had a small northeastward component. Currents were onshore at mid-depth. Temperature, salinity and sigma-t (as indicated by the SEACATs) were almost uniform in depth at T = 28.8 deg, S = 35.6* psu, and sigma-t = 22.5. The current flowing northward near bottom suggests the presence of a northward-acting pressure gradient force, since the alongshelf wind stress component was opposite.

During the upwelling favorable period (Table 6b), the magnitude of the northeastward current increased by a factor of three. Currents at both levels had an offshore component. This seems puzzling at first, but one must view the chosen coordinate orientation (-50 deg) with caution when considering the algebraic sign of the cross-shelf current components. The local topography (Fig. 1a) has shallow-relief ridges and swales running almost east-west which may steer the currents, particularly those closest to bottom. Had we rotated the coordinate system to conform more closely to local bathymetry, the cross-shelf currents during the upwelling period would be onshore, thus conforming to expectations. This emphasizes how difficult it is to define precisely the sign of cross-shelf flow from individual measuring locations.

Temperature, salinity and sigma-t changed slightly during the upwelling period. Consistent with upwelling conditions, a slight change in salinity and sigma-t was noted reflecting either the offshore advection of lower salinity surface water nearer the coast or onshore advection of higher salinity offshore water near bottom to M2. Thus, while temperature was a uniform 29.1 C at M2, mean salinity was 35.6/35.7 psu at 6.5/12.5 below surface.

---

* All salinities are reported on the practical salinity scale.

The 40hlp currents in the inlet are difficult to interpret (see Blanton et al. 1994 for discussion). We will rely on subsurface pressure fluctuations to discern sub-tidal frequency fluxes of water through the inlet and will not discuss further the 40hlp current meter data from M1.

3.3 Time series of winds, currents, and water mass properties

Plots of the 3hlp and 40hlp moored data display the rotated wind stress and current components, as well as temperature, salinity, σ_t and subsurface pressure data (Figs. 6 - 11). The 3hlp currents at M1 (Fig. 6) showed strong tidal currents of about 100 cm/s along the axis of the inlet (x component). Positive x-component currents ebb toward the ocean and were only slightly smaller near bottom. The cross-inlet fluctuations were comparatively small (note differences in scale) when compared to the axial fluctuations. Cross-inlet components are difficult to interpret because small changes in the coordinate rotation could change the algebraic sign. Therefore, the interpretation of cross-axis current components in the inlet will be deferred until further analyses are completed.

Tidal currents at M2 were strongest in the cross-shelf (x) component (Fig. 7). They also were embedded in the alongshelf (y) component to a smaller degree. This is characteristic of tidal current vectors on the continental shelf of the southeastern U.S. (Pietrafesa et al. 1985), which trace out elongated ellipses in coastal waters with major axes usually perpendicular to shore. Note the displacement of the oscillating y component currents above zero beginning 1 September, which coincides with the onset of upwelling favorable wind stress (Fig. 7). This will be discussed in more detail for the 40hlp data.

Temperature, salinity, and σ_t fluctuations in the inlet (M1) show the effects of tidal currents as they advect horizontal gradients of properties past the sensors (Fig. 8). Note the absence of strong fluctuations at M2. The similarity in the top and bottom data indicates that the water column essentially is vertically homogeneous, although slight differences do occur offshore at M2 after the onset of upwelling.

The relative magnitude of horizontal gradients of temperature and salinity at M1 and M2 were estimated based on the 3hlp statistics for neap and spring tides (Table 7). The gradients were derived from a one-dimensional model for concentration, or

$$\frac{dC}{dt} + u\frac{dC}{dx} = 0$$

where u is the rms amplitude of horizontal tidal velocity along the principal axis, and d[C]/dt is the time rate of change in the property over one-half of a tidal cycle (6.24 hr). Only mid-water column data were used in these estimates. Temperature gradients in the inlet were 0.04/0.03 C/km during neap/spring tides respectively. Offshore at M2, the corresponding gradients were 0.07/0.05 C/km for neap/spring tides respectively. An offshore hydrographic survey at neap tide (discussed later) indicated that the temperature gradient was about 0.08 deg C/km.

Salinity gradients at M1 based on the above equation were 0.07 and 0.05 psu/km during neap and spring tides. Offshore at M2, the corresponding gradients were 0.03/0.03 psu/km for neap/spring tides respectively. The neap tide hydrographic survey indicated a salinity gradient near M2 of 0.02 psu/km. In summary, horizontal temperature gradients were somewhat greater offshore than at the inlet, while salinity gradients were significantly weaker at the offshore location.

The 40hlp data for wind stress and currents off the coast at mooring M2 (Fig. 9) show the effects of wind on coastal currents. The upwelling favorable wind regime (1 - 6 September) generated northeastward currents at M2 (TOP and BOT). Note that these currents were present with significantly less strength before the onset of upwelling (except for a brief interlude on 30-31 August). Short period fluctuations in wind stress are evident in the 3hlp data that are filtered out in the 40hlp data (compare Fig. 6a to Fig. 10a). The short-period wind fluctuations appeared to have an important effect on water properties and currents during NED1 (Blanton et al. 1994a) but the response to short-period wind fluctuations during NED2 is not obvious.

During the upwelling event, waters at M1 and M2 were weakly stratified (Fig. 11). This is consistent with the onshore transport of higher density water from offshore near bottom and/or corresponding offshore transport of lower density coastal water near the surface.

The evolution of temperature, salinity and density fields at M1 and M2 is easily seen in the 40hlp data (Fig. 11). Water offshore was slightly cooler by about 0.5 C, but this difference had almost disappeared by 4 September. Salinity was consistently lower at M1 by about 2 psu yielding an overall salinity gradient of about 0.08 psu/km (also see Table 6). The corresponding density gradient was about 6.2×10^{-5} kg/m^4. An increase in sigma-t began in the inlet on 3 September and a corresponding increase at M2 began about one day later. These increases were probably caused by the advection of lower temperature and higher salinity water into the region.

Subsurface pressure (SSP) fluctuations (Fig. 11d) were substantially weaker during NED2 than during NED1 (Blanton et al. 1994a) reflecting the weaker wind forcing. The expected drop in SSP during the onset of upwelling did not occur. Instead, SSP remained high corresponding with an onshore wind stress component, until this component disappeared.

3.4 Offshore hydrographic sections

Periodic offshore surveys were conducted with a hiatus in sampling when Hurricane Emily passed offshore (Fig. 3). The following figures consist of cross-shelf versus depth plots of salinity, chlorophyll *a*, temperature and σ_t for each of the NED2 offshore surveys. Tables of bin-averaged data from which these plots are drawn are available from the authors upon request. The ODIS flow-through system also allowed us to tie in the near-surface estuarine data to similar data offshore as well as help resolve scales of variation. We have divided this section into surveys that were done under calm wind stress conditions and compared them to those conducted during the upwelling regime.

3.4.1 Offshore surveys LW1, HW1, OS1 and OS2 (25-29 Aug 1993)

These surveys (Figs. 12-15) were conducted under calm wind conditions. LW1 and HW1 surveys (Fig. 12, 13) were done within about 6 hours of each other in order to define the effects of the tides on hydrographic structure from low-water slack to high-water slack. Winds were weakly downwelling favorable and onshore during these two surveys, and shelf waters were vertically mixed all across the survey region, consistent with downwelling conditions. Isopleths on all variables were advected onshore about 2 km from the time of the low-water survey until high water. Maximum chl *a* concentrations were found near the edge of the inlet's delta, as was the case in NED1 (Blanton et al. 1994a).

Wind stress had diminished to almost calm conditions during OS1 (Northern transect) and OS2 (Southern transect). The isolines of salinity and sigma-t in OS1 (Fig. 14) indicated some weak vertical stratification, which is consistent with wind relaxation causing offshore tilting near surface in the coastal frontal zone located between stations S2 and S8. Highest chl *a* was observed near bottom at the shallowest station (S0). Similarly, weak stratification was observed during OS2 (Fig. 15) along the northern transect and along the delta's arc (Stations N0 - A6). Note the high chl *a* observed at bottom on the northern transect near N2.

3.4.2 Offshore surveys OS3 and OS4 (2-3 September 1993)

These two surveys (Figs. 16 and 17) were completed during upwelling favorable winds at or immediately after spring tide. An onshore component of wind stress also was a factor during both surveys. The coastal front was well-mixed and the salinity and density gradients were uniform across both the northern and southern transects. The maximum in chl *a* was located at bottom at the shallowest stations observed (S0 and N1). Apparently, sufficient vertical mixing through wind stress and tidal currents prevented vertical stratification from forming in the coastal front.

3.4.3 Offshore surveys OS5 through OS7 (5-8 September 1993)

OS5 (Fig. 18) was conducted during upwelling favorable winds, but these had disappeared by the time of OS6 and OS7 (Figs. 19 and 20). Upwelling winds had blown for over two days previous to OS5, and the coastal front (Fig. 18) exhibited significant vertical stratification. Chl *a* concentrations were lower than observed on previous surveys. Vertical stratification was still present in the bottom half of the coastal front during OS6 (Fig. 19), and chl *a* concentrations had increased near bottom at Station N0. By the time of OS7 (Fig. 20), vertical stratification had diminished slightly.

3.5 Estuarine longitudinal sections

A high water and low water survey from the North Edisto inlet mouth to 23 km inland (Fig. 1b) was conducted on 5 September. The high-water survey (Fig. 21) showed a well-mixed estuary with salinities greater than 34 PSU at the mouth decreasing to less than 31 PSU at the upstream survey limit. There was weak vertical stratification in temperature and salinity at the mouth, representing oceanic conditions that had been advected in on the flooding tide. The cooler, higher salinities that were advected over the delta by the flooding tide induced a relatively strong vertical stratification. The horizontal salinity gradient was significantly less than was observed during NED1 (Blanton et al. 1994a). At the following low-water survey (Fig. 22), the estuary was weakly stratified by the advection of relatively low density water by the ebbing tide. The 31 PSU isohaline had been translated about 6 km over the half tidal cycle. Chl *a*, uniformly high for each survey with concentrations between (6-7 µg/l), increased slightly with depth.

3.6 Throat surveys

South (S), Middle (M) and North (N) inlet stations (near M1 in Fig. 1a) were sampled as quickly as possible for each of the nine throat surveys. All CTD casts and plankton tows were taken only during flood tides at night. The order of station selection was random and if time permitted, the three

stations were repeated. A preliminary look at the hydrographic data suggests slight lateral variability of the water mass properties in the throat cross-section. However, we need to examine the data more closely since the casts were taken at different times relative to maximum flood, and tidal aliasing (especially with such strong tidal currents) may confound the relevant features.

An additional CTD cast (sometimes without a plankton tow) was taken at the middle throat station at maximum flood tide whenever possible. A temporal plot of these CTD measurements (Fig. 23) revealed temporal fluctuations in salinity and a general decrease in temperature over the last half of the survey. The absence of data on the plot is due to the hiatus in throat surveys between 29 Aug and 2 September. Chl *a* exhibited a pattern of increasing concentration with depth (Fig. 23c). Beginning on 2 September, chl *a* decreased from 7 to 4 mg/l over a four-day period, with declines which began first in near-surface waters and then extended to greater depth.

3.7 Plankton Results

The spatial distribution of chl *a* in offshore surveys was quite similar throughout the study period. Generally, chl *a* was highest near bottom at the shallow stations near the arc, and decreased with distance offshore (e.g., Fig. 14). Concentrations typically ranged from 4-6 µg/l nearshore to 0.5-1 µg/l offshore. Chl *a* concentrations were inversely proportional to salinity (Fig. 24a). Since salinity was the major contributor to water density, chl *a* fluorescence also was inversely proportional to σ_t (Fig. 24b). Optical backscatter (OBS) measured by the CTD was positively correlated with chl *a* fluorescence (Fig. 24c).

These observations indicate that the major source of phytoplankton biomass in inner shelf waters was from estuarine or arc waters. This higher signal was diluted by mixing with more saline offshore waters which contained less phytoplankton. A similar spatial pattern was observed in the offshore surveys during the first study period in summer 1993. The small variance in optical backscatter (OBS) at low chl *a* concentrations (i.e., in offshore samples), the exponential increase in OBS with increasing

phytoplankton biomass, and the greater variance in OBS at high chl *a* (Fig. 24c) all suggest that phytoplankton is a more significant component of suspended particles offshore, while inshore inorganic and other organic particles (e.g., detritus) assume greater importance.

The relationships observed between hydrography and chl *a* in offshore waters (Fig. 24) do not hold for samples from the estuary throat (Fig. 25), even though the dynamic range in salinity is greater there. (OBS was rarely measured in the estuary throat stations.) These data imply that chl *a* did not increase monotonically up the estuary (i.e., with decreasing salinity), or that upstream waters were not the only local source of chl *a*. Other possibilities include sessile algae flushed from salt marshes, and benthic phytoplankton resuspended from the sediment-water surface via tidal mixing (see below). Whatever the source, the absence of predictable relationships between chl *a* and salinity or sigma-t in the estuary throat directly reflects the generally observed vertical stratification in chl *a* (i.e., increasing with depth) in waters which were hydrographically well-mixed.

Generally, vertical gradients in chl *a* cannot be maintained in the presence of strong vertical mixing. Yet, such gradients in pigments were invariably observed (Figs. 12-22) in hydrographically well-mixed waters. In fact, the greatest vertical gradients generally occurred in the shallowest and therefore presumably most mixed waters. This implies that the source of the pigment signal was apparently not gravitational settling of pelagic phytoplankton, but likely resuspension of benthic taxa. In 1993, however, we only sampled during flood tides and we did not collect samples for microscopic observations, hence this hypothesis could not be evaluated at that time. Sampling was modified in 1994 to explore this hypothesis, the results of which will be reported later.

3.8 Larval results

Densities of penaeid postlarvae and blue crab megalopae were considerably greater in surface plankton tows than in those made near bottom in the inlet throat (Fig. 26). Prior to the August 28 peak in penaeid postlarvae density, the wind had been downwelling favorable for several days, and

significant onshore wind stress existed prior to the start of sampling. Although the downwelling wind event immediately preceding this peak of postlarvae was not particularly large, the onshore component was consistent during the period. Density of blue crab megalopae also increased during this two-day period (Fig. 26b). Sampling was suspended on August 29 due to a hurricane threat and was not resumed until September 2. The peaks of megalopal densities (2-3 days after the full moon) coincided with strong winds which were upwelling favorable with an onshore cross-shelf component. These persisted until September 6, after which winds were calm.

4.0 Summary

The first five days of wind stress during NED2 were weak, downwelling favorable, with an onshore component. Coastal waters were weakly stratified to well mixed during that period (Figs. 12-15). Low frequency coastal currents at M2 were northward at less than 5 cm/s (Fig. 9). As wind changed to upwelling favorable for the next six days, the currents at M2 increased by a factor of 3. Coastal waters continued to be vertically well mixed (Fig. 16-17), presumably because wind stress and spring tidal currents were strong enough to prevent stratification. After wind stress diminished, coastal waters became weakly stratified (Fig. 18-19).

4.1 Preliminary interpretation

A combined transect using the R/V ANITA and R/V BLUE FIN was conducted 5 September. This transect extended from Station 6 in the North Edisto Estuary to a station 22 km offshore of the inlet delta (Fig. 27). Strongest horizontal salinity gradients were observed in the estuary and across the delta. The salinity front through the delta separated high chl *a* concentrations in the estuary (> 7 mg/l) from lower values of 3 mg/l or less in the ocean. Strong horizontal gradients in salinity and chlorophyll-a in the shallow delta suggest that circulation processes significantly inhibit

communications between ocean and inlet. Channels along the flanks of the shoals as well as the channel through the throat provide the principal flow routes connecting ocean and estuary.

Salinities along the arc (represented by Stations S1, A6, and N1) usually were minimum at the shallowest northern and southern stations. Maximum vertical stratification was observed during relatively calm winds (OS1, OS2) but became well-mixed during strong winds (OS3, OS4). Weak stratification reappeared (OS5, OS6) as wind strength diminished. Salinity along the arc (and at M1 and M2) increased during upwelling winds and decreased during downwelling winds which suggests a low-salinity source farther north.

Penaeid and *Callinectes sapidus* (Fig. 26) abundance data in the inlet throat suggests that onshore wind stress plays an important role in the transport to estuaries, perhaps rivaling in importance the hypothesized role of downwelling winds. The most efficient wind component is downwelling winds with an onshore component. During NED1 (Fig. 28), prolonged ingress of penaeid larvae began 21 May and lasted four days (Blanton et al. 1994a). Downwelling winds with an offshore component were noted during the first two days followed by upwelling winds with an onshore component. Abundances were marginally greater in bottom samples after the onshore winds began. This was followed by the largest ingress event of NED1 which occurred during downwelling winds with an onshore component.

Consideration of NED2 results (Fig. 26) reinforces the importance of onshore winds in shallow water where transport is more directly downward. Simultaneous ingress of *Penaeid* and *Callinectes sapidus* larvae occurred during the single large *upwelling* event during which the wind had a significant onshore component. Thus, NED1 and NED2 results suggest that winds blowing onshore, regardless of the direction of the alongshelf component, provide an effective circulation regime for ingress of larvae into estuaries.

Independent of whether winds were upwelling or downwelling favorable, profiles of

phytoplankton fluorescence invariably showed little vertical structure offshore but a strong near-bottom maxima associated with the shallow arc. Thus horizontal gradients were the dominant feature of chl *a* distributions in shelf waters, while vertical gradients were greater at the entrance to the estuary. This pattern suggests that the estuary-delta was the local source of phytoplankton to shelf waters, and that gradients in phytoplankton distribution could be maintained even in the presence of strong vertical mixing. The source(s) of gradient maintainance is presently unknown. However, shallow-water hydrodynamics, governed by time scales from seconds to hours, appear to be strongly linked to the high productivity of these waters, as observed in adjacent Georgia waters (Verity et al. 1993). Phytoplankton biomass increases dramatically along the arcuate delta in front of the estuary during flood tides. Thus the ocean-estuary interface possibly acts as a nutritional hypodermic, injecting food into the water carrying the larvae as it advects into the estuary.

5.0 References

Blanton, J. O. 1986. Coastal frontal zones as barriers to offshore fluxes of contaminants. Rapp. P. -v. Reun. Cons. int. Explor. Mer 186: 18-30.

Blanton, J. O. and L. P. Atkinson. 1983. Transport and fate of river discharge on the continental shelf of the southeastern United States. J. Geophys. Res., 88(C8): 4730-4738.

Blanton, J. O., L.-Y. Oey, J. Amft, and T. N. Lee. 1989a. Advection of momentum and buoyancy in a coastal frontal zone. J. Phys. Oceanogr. 19: 98-115.

Blanton, J. O., J. A. Amft, D. K. Lee, and A. Riordan. 1989b. Wind stress and heat fluxes observed during Winter and Spring, 1986. J. Geophys. Res. 94: 10,686-10,698.

Blanton, J.O., Julie Amft and P.G. Verity. 1994a. The May 1993 North Edisto Ingress Experiment (NED1). Technical Report 94-1, Georgia Marine Science Center, University System of Georgia. Savannah, GA. 72 pp.

Blanton, J. O., F. Werner, C. Kim, L. Atkinson, T. Lee and D. Savidge. 1994b. Transport and fate of low-density water in a coastal frontal zone. Cont. Shelf Res., 14: 401-427.

Blanton, J. O., E. Wenner, F. Werner and D. Knott. 1995. Effects of wind-generated coastal currents on the transport of blue crab megalopae on a shallow continental shelf. Bull. Mar. Sci., 57: 739-752.

Christmas, J. Y. and D. J. Etzold. 1977. The shrimp fishery of the Gulf of Mexico United States; a regional management plan. Gulf Coast Res. Lab. Tech. Rep. Ser. No. 2. 125 pp.

Cook, H. L. and M. A. Murphy. 1969. The culture of larval penaeid shrimp. Trans. Am. Fish. Soc. 98(4): 751-754.

Dobkin, S. 1961. Early developmental stages of pink shrimp, *Penaeus duorarum*, from Florida waters. U.S. Fish Wildl. Serv. Fish. Bull. 190(61): 321-349.

Holliday, D. V. 1992. Acoustical measurement of zooplankton from moorings. International Council for the Exploration of the Sea. Document C. M. 1992/B:7. 5 pp.

Pietrafesa, L. J., J. O. Blanton, J. D. Wang, V. Kourafalou, T. N. Lee, K. A. Bush. The tidal regime in the South Atlantic Bight, in Oceanography of the Southeastern United States Continental Shelf, Coastal Estuarine Sci., Vol. 2, AGU, Washington, D.C., p. 63-76.

Verity, P. G., J. A. Yoder, S. S. Bishop, J. R. Nelson, D. B. Craven, J. O. Blanton, C. Y. Robertson, and C. R. Tronzo. 1993. Composition, productivity and nutrient chemistry of a coastal ocean planktonic food web. Cont. Shelf Res. 13: 741-776.

Yoder, J. A., P. G. Verity, S. S. Bishop, and F. E. Hoge. 1993. Phytoplankton chl *a*, primary production, and nutrient distributions across a coastal frontal zone off Georgia, USA. Cont. Shelf Res. 13: 131-141.

TABLE 1. Moored instrumentation used during NED2

AUGUST/SEPTEMBER 1993 MOORING INFORMATION FOR THE NORTH EDISTO STUDY (NED2)

STATION	INSTRU. DEPTH (m)	WATER DEPTH (m)	INSTRUMENT	PARAMETERS MEASURED	DEPLOYMENT DATES (1993)	LATITUDE (deg N)	LONGITUDE (deg W)
M1	-9.5	-17.5	SEACAT 295	C,T	08/26 - 09/07	32.566	80.191
M1	-11.0	-17.5	S4 706	C,T,V	08/26 - 09/07	32.566	80.191
M1	-15.0	-17.5	S4 1530	C,T,V	08/26 - 09/07	32.566	80.191
M1	-16.5	-17.5	SEACAT 849	C,P,T	08/26 - 09/07	32.566	80.191
M2	-6.5	-13.5	SEACAT 327	C,T	08/26 - 09/07	32.416	80.074
M2	-7.5	-13.5	S4 908	C,T,V	08/26 - 09/07	32.416	80.074
M2	-11.0	-13.5	S4 909	C,T,V	08/26 - 09/07	32.416	80.074
M2	-12.5	-13.5	SEACAT 848	C,P,T	08/26 - 09/07	32.416	80.074
FBIS1	+9.8	land	C-MAN	A,B,W	08/23 - 09/09	32.68	79.89
SVLS1	+32.9	-14.0	C-MAN	A,B,W	08/23 - 09/09	31.95	80.68

Instrument:

SEACAT serial# = Sea-Bird Electronics SEACAT data logger
S4 serial# = InterOcean Systems S4 current meter

Weather Stations:

FBIS1 = Folly Beach (C-MAN)
SVLS1 = Savannah Light Tower (C-MAN)

C-MAN = Coastal-Marine Automated Network (NOAA)

Parameters:

A = air temperature
B = barometric pressure
C = conductivity
P = subsurface pressure
T = water temperature
V = current velocity
W = wind velocity

TABLE 2. Conductivity, temperature, depth (CTD) station information for NED2 from R/V BLUE FIN.

	Cruise	Cast #	Sta	Date mm dd yy	Time (EDT)	Water Depth (m)	Latitude (N) deg min		Longitude (W) deg min	
				Offshore Low Water Water Survey: (lw)						
	B2	001	N0	08/25/93	0746	4.9	32	33.93	80	07.87
	B2	002	N2	08/25/93	0819	8.5	32	32.26	80	06.28
	B2	003	N4	08/25/93	0848	11.3	32	30.76	80	04.84
	B2	004	N6	08/25/93	0921	9.4	32	29.24	80	03.35
	B2	005	N9	08/25/93	0948	10.9	32	27.67	80	01.70
	B2	006	N12	08/25/93	1037	13.7	32	24.60	79	58.72
				Offshore Low Water Water Survey: (hw)						
	B2	007	N12	08/25/93	1339	14.9	32	24.66	79	58.64
	B2	008	N9	08/25/93	1412	14.5	32	26.97	80	01.08
	B2	009	N6	08/25/93	1449	11.5	32	29.31	80	03.36
	B2	010	N4	08/25/93	1513	13.0	32	30.84	80	04.94
	B2	011	N2	08/25/93	1542	10.0	32	32.34	80	06.37
	B2	012	N0	08/25/93	1606	5.6	32	33.88	80	07.85
				Throat Survey #1: (ts1)						
xx	B2	013	M	08/27/93	0046	12.2	32	34.53	80	12.04
xx	B2	014	N	08/27/93	0147	12.2	32	34.61	80	12.00
	B2	015	M	08/27/93	0228	21.3	32	34.33	80	11.78
xx	B2	016	S	08/27/93	0239	16.4	32	34.44	80	12.09
xx	B2	017	N	08/27/93	0329	10.7	32	34.65	80	12.03
xx	B2	018	S	08/27/93	0407	15.9	32	34.45	80	12.17
xx	B2	019	M	08/27/93	0450	13.1	32	34.57	80	12.08
				Offshore Transect Survey #1: (os1)						
	B2	020	S0	08/27/93	2031	5.3	32	31.01	80	14.14
	B2	021	S4	08/27/93	2121	11.2	32	27.78	80	11.02
	B2	022	S6	08/27/93	2143	11.5	32	26.26	80	09.51
	B2	023	S12	08/27/93	2241	17.0	32	21.70	80	04.98
	B2	024	S10	08/27/93	2316	12.0	32	23.16	80	06.48
++	B2	025	S8	08/27/93	2340	11.2	32	24.72	80	08.01
	B2	026	S6	08/28/93	0022	10.9	32	26.29	80	09.52
++	B2	027	S4	08/28/93	0045	10.6	32	27.81	80	11.05
++	B2	028	S2	08/28/93	0125	9.5	32	29.45	80	12.69
	B2	029	S0	08/28/93	0220	5.1	32	30.96	80	14.22
++	B2	030	A6	08/28/93	0313	8.5	32	30.58	80	08.58
				Offshore Transect Survey #2: (os2)						
	B2	031	N0	08/28/93	2119	4.5	32	33.93	80	07.68
	B2	032	N2	08/28/93	2141	8.5	32	32.31	80	06.24
	B2	033	N4	08/28/93	2204	11.5	32	30.84	80	04.75
	B2	034	N8	08/28/93	2242	11.0	32	27.71	80	01.78
	B2	035	N12	08/28/93	2326	13.5	32	24.69	79	58.54
	B2	036	N9	08/28/93	0038	13.5	32	26.98	80	00.98
++	B2	037	N6	08/29/93	0112	10.0	32	29.30	80	03.23
	B2	038	N4	08/29/93	0155	11.5	32	30.79	80	04.78
++	B2	039	N2	08/29/93	0218	8.6	32	32.43	80	06.36
++	B2	040	N0	08/29/93	0320	5.5	32	33.88	80	07.92
++	B2	041	A6	08/29/93	0425	8.0	32	30.54	80	08.74
				Offshore Transect Survey #3: (os3)						
	B2	042	S0	09/01/93	2327	5.8	32	31.06	80	14.10
	B2	043	S2	09/01/93	2356	10.5	32	29.35	80	12.50
	B2	044	S4	09/02/93	0017	11.2	32	27.83	80	10.99
	B2	045	S8	09/02/93	0059	11.9	32	24.70	80	07.93
	B2	046	S12	09/02/93	0142	17.6	32	21.71	80	04.97
++	B2	047	S9	09/02/93	0235	12.6	32	24.15	80	07.25
	B2	048	S6	09/02/93	0405	12.4	32	26.40	80	09.40
++	B2	049	S4	09/02/93	0429	9.5	32	27.90	80	11.10
++	B2	050	S2	09/02/93	0540	9.7	32	29.40	80	12.70
	B2	051	S0	09/02/93	0640	5.8	32	31.09	80	14.11
	B2	052	A6	09/02/93	0725	8.5	32	30.54	80	08.63
				Offshore Transect Survey #4: (os4)						
	B2	053	N0	09/02/93	2346	7.0	32	34.04	80	07.77
	B2	054	N2	09/03/93	0014	9.5	32	32.32	80	06.26
	B2	055	N4	09/03/93	0042	12.0	32	30.83	80	04.72
	B2	056	N8	09/03/93	0125	11.5	32	27.77	80	01.64
++			N12		0311			** NO CTD CAST		
	B2	057	N9	09/03/93	0403	13.7	32	26.95	80	00.94
	B2	058	N6	09/03/93	0440	10.2	32	29.38	80	03.26
++	B2	059	N4	09/03/93	0505	11.4	32	30.92	80	04.85
	B2	060	N2	09/03/93	0610	8.7	32	32.41	80	06.38
++	B2	061	N1	09/03/93	0635	6.9	32	33.13	80	07.23
++	B2	062	A6	09/03/93	0805	8.7	32	30.51	80	08.63
				Offshore Transect Survey #5: (os5)						
	B2	063	S2	09/05/93	1340	10.4	32	29.32	80	12.45
	B2	064	S5	09/05/93	1423	14.2	32	27.05	80	10.27
	B2	065	S8	09/05/93	1452	11.9	32	24.71	80	07.92
	B2	066	S12	09/05/93	1531	17.4	32	21.72	80	04.94
	B2	067	S9	09/05/93	1635	13.2	32	23.97	80	07.16
++	B2	068	S6	09/05/93	1708	10.9	32	26.29	80	09.52
++	B2	069	S4	09/05/93	1838	10.6	32	27.83	80	11.04
++	B2	070	S1	09/05/93	1957	7.7	32	30.05	80	13.38
	B2	071	S0	09/05/93	2042	5.7	32	31.02	80	14.19
++	B2	072	A6	09/05/93	2130	9.0	32	30.55	80	08.52
				Offshore Transect Survey #6: (os6)						
	B2	073	N2	09/06/93	1413	9.5	32	32.30	80	06.19
	B2	074	N5	09/06/93	1442	14.0	32	30.04	80	03.96
	B2	075	N8	09/06/93	1511	11.6	32	27.68	80	01.68
	B2	076	N12	09/06/93	1546	13.8	32	24.64	79	58.60
++	B2	077	N8	09/06/93	1704	11.3	32	27.70	80	01.73
++	B2	078	N6	09/06/93	1759	10.4	32	29.30	80	03.29
	B2	079	N4	09/06/93	1913	11.5	32	30.89	80	04.98
	B2	080	N2	09/06/93	1934	8.8	32	32.41	80	06.36
++	B2	081	N1	09/06/93	1954	7.0	32	33.24	80	07.03
	B2	082	N0	09/06/93	2035	5.7	32	33.94	80	07.86
				Offshore Transect Survey #7: (os7)						
	B2	084	S12	09/07/93	1717	17.7	32	21.70	80	05.09
	B2	085	S9	09/07/93	1747	13.8	32	24.03	80	07.28
	B2	086	S7	09/07/93	1812	14.0	32	25.49	80	08.74
++	B2	087	S5	09/07/93	1917	13.7	32	27.13	80	10.30
++	B2	088	S3	09/07/93	2017	11.1	32	28.59	80	11.94
++	B2	089	S1	09/07/93	2122	7.2	32	30.20	80	13.46
	B2	090	S0	09/07/93	2209	5.7	32	31.06	80	14.15
++	B2	091	A6	09/07/93	2257	8.4	32	30.55	80	08.64

x = 5 minute plankton net tows were taken (by MRRI) at this station
+ = 10 minute plankton net tows were taken (by MRRI) at this station

(a '+' or 'x' in column 1 designates a surface tow;
a '+' or 'x' in column 2 designates a near bottom tow)

Cruise: B2 = R/V *BLUE FIN* (NED2: Aug 93 cruise)

Station: S = south side of channel (near Edisto Island)
M = middle of channel (in throat)
N = north side of channel (near Privateer Point)

N# = offshore transect station (North)
S# = offshore transect station (South)
A# = offshore arc station

TABLE 3. Conductivity, temperature, depth (CTD) station information for NED2 from R/V ANITA.

	Cruise	Cast #	Sta	Date mm dd yy	Time (EDT)	Water Depth (m)	Latitude (N) deg min		Longitude (W) deg min	
				Throat Survey #2: (ts2)						
xx	A2	001	M	08/28/93	0025	19.8	32	34.21	80	11.46
xx	A2	002	S	08/28/93	0115	15.5	32	34.28	80	11.71
xx	A2	003	N	08/28/93	0155	14.3	32	34.41	80	11.60
xx	A2	004	S	08/28/93	0235	13.1	32	34.22	80	11.71
xx	A2	005	M	08/28/93	0320	13.4	32	34.41	80	11.65
xx	A2	006	N	08/28/93	0400	17.7	32	34.23	80	11.42
				Throat Survey #3: (ts3)						
xx	A2	007	N	09/02/93	0343	15.8	32	34.29	80	11.53
xx	A2	008	M	09/02/93	0423	14.6	32	34.23	80	11.59
xx	A2	009	S	09/02/93	0459	12.8	32	34.22	80	11.72
				Throat Survey #4: (ts4)						
xx	A2	010	N	09/02/93	2051	17.1	32	34.37	80	11.52
xx	A2	011	S	09/02/93	2135	15.8	32	34.26	80	11.68
xx	A2	012	M	09/02/93	2204	15.2	32	34.28	80	11.62
xx	A2	013	M	09/03/93	0440	12.8	32	34.25	80	11.59
xx	A2	014	S	09/03/93	0532	14.9	32	34.24	80	11.64
xx	A2	015	N	09/03/93	0605	15.5	32	34.32	80	11.47
	A2	016	M	09/03/93	0630	19.8	32	34.22	80	11.46
				Throat Survey #5: (ts5)						
xx	A2	017	M	09/03/93	2038	15.8	32	34.26	80	11.64
xx	A2	018	N	09/03/93	2105	17.4	32	34.32	80	11.50
xx	A2	019	S	09/03/93	2140	14.3	32	34.23	80	11.71
				Throat Survey #6: (ts6)						
xx	A2	020	M	09/04/93	2004	14.0	32	34.26	80	11.62
xx	A2	021	S	09/04/93	2031	12.5	32	34.08	80	11.53
xx	A2	022	N	09/04/93	2056	20.4	32	34.26	80	11.46
				Inshore High Water Survey: (hw)						
	A2	023	NED1	09/05/93	0956	11.0	32	32.73	80	09.73
	A2	024	NED2	09/05/93	1013	21.0	32	32.08	80	11.29
	A2	025	NED3	09/05/93	1038	10.4	32	36.23	80	13.94
	A2	026	NED4	09/05/93	1056	7.3	32	37.45	80	15.85
	A2	027	NED5	09/05/93	1114	10.8	32	39.14	80	14.26
	A2	028	NED6	09/05/93	1134	12.3	32	40.91	80	13.32
				Inshore High Water Survey: (lw)						
	A2	029	NED1	09/05/93	1555	9.8	32	32.64	80	09.50
	A2	030	NED2	09/05/93	1616	16.5	32	33.79	80	10.96
	A2	031	NED3	09/05/93	1652	10.8	32	36.15	80	13.81
	A2	032	NED4	09/05/93	1716	8.3	32	37.45	80	15.85
	A2	033	NED5	09/05/93	1739	8.8	32	39.15	80	14.28
	A2	034	NED6	09/05/93	1800	6.3	32	40.89	80	18.38
				Throat Survey #7: (ts7)						
	A2	035	M	09/05/93	2024	13.7	32	34.27	80	11.59
xx	A2	036	S	09/05/93	2038	13.4	32	34.17	80	11.63
xx	A2	037	N	09/05/93	2108	17.3	32	34.26	80	11.49
xx	A2	038	M	09/05/93	2142	15.8	32	34.18	80	11.51
xx	A2	039	S	09/05/93	2208	13.4	32	34.16	80	11.56
xx	A2	040	N	09/05/93	2236	18.6	32	34.28	80	11.49
xx	A2	041	M	09/05/93	2303	14.3	32	34.27	80	11.62
				Throat Survey #8: (ts8)						
xx	A2	042	M	09/06/93	2047	15.6	32	34.22	80	11.62
xx	A2	043	N	09/06/93	2110	15.8	32	34.37	80	11.59
xx	A2	044	S	09/06/93	2135	13.5	32	34.18	80	11.61
xx	A2	045	N	09/06/93	2202	16.9	32	34.32	80	11.49
xx	A2	046	S	09/06/93	2228	14.3	32	34.23	80	11.71
xx	A2	047	M	09/06/93	2253	14.3	32	34.30	80	11.66
				Throat Survey #9: (ts9)						
xx	A2	048	S	09/07/93	2026	12.5	32	34.15	80	11.63
xx	A2	049	N	09/07/93	2105	15.5	32	34.22	80	11.47
xx	A2	050	M	09/07/93	2130	15.5	32	34.27	80	11.64
xx	A2	051	M	09/07/93	2154	15.7	32	34.30	80	11.70
xx	A2	052	S	09/07/93	2218	13.4	32	34.23	80	11.70
xx	A2	053	N	09/07/93	2243	15.5	32	34.26	80	11.47

x = 5 minute plankton net tows were taken (by MRRI) at this station

(an 'x' in column 1 designates a surface tow;
an 'x' in column 2 designates a near bottom tow)

Cruise: A2 = R/V *ANITA* (NED2: Aug 93 cruise)

Station: S = south side of channel (near Edisto Island)
M = middle of channel (in throat)
N = north side of channel (near Privateer Point)

NED# = estuarine station in North Edisto River

TABLE 4. First order statistics for parameters measured during NED2. The station location and depth above bottom are designated for each sensor. All vectors with x and y components have the coordinate system rotated 50 degrees clockwise. All series were 12.75 days long and began 25 August 1993 at 18 hr GMT and ended 7 September 1993 at 12 hr GMT. (a) 3hlp data; (b) 40hlp data.

Parameter	Min	Max	Mean	Stan. Dev.
(a) 3-HOUR LOW-PASS (3hlp) DATA:				
FBIS1 barometric pressure (mb)	1011.88	1022.04	1017.23	2.48
FBIS1 air temperature (° C)	24.48	30.44	27.87	1.36
FBIS1 x-comp wind stress (Pa*10)	-0.77	0.15	-0.13	0.15
FBIS1 y-comp wind stress (Pa*10)	-0.62	0.82	0.14	0.27
SVLS1 barometric pressure (mb)	1012.10	1021.72	1016.94	2.28
SVLS1 air temperature (° C)	23.98	28.51	27.29	0.86
SVLS1 east wind stress (Pa*10)	-0.77	0.34	-0.20	0.21
SVLS1 north wind stress (Pa*10)	-0.79	0.77	0.04	0.24
M1 8.0m temperature (° C)	28.47	30.50	29.34	0.40
M1 8.0m salinity (PSU)	32.27	34.35	33.56	0.52
M1 8.0m sigma-t (kg/m^3)	19.97	21.66	20.87	0.43
M1 6.5m x-comp current (cm/s)	-93.71	126.81	7.50	71.79
M1 6.5m y-comp current (cm/s)	-37.17	28.78	-0.64	16.98
M1 2.5m x-comp current (cm/s)	-80.28	105.10	5.37	58.27
M1 2.5m y-comp current (cm/s)	-27.25	33.55	0.36	15.09
M1 1.0m temperature (° C)	28.46	30.54	29.32	0.42
M1 1.0m salinity (PSU)	32.33	34.42	33.58	0.51
M1 1.0m sigma-t (kg/m^3)	19.98	21.61	20.89	0.42
M1 1.0m pressure (dbar)	15.70	17.66	16.65	0.58
M2 7.0m temperature (° C)	28.48	29.46	28.97	0.22
M2 7.0m salinity (PSU)	35.24	35.96	35.59	0.18
M2 7.0m sigma-t (kg/m^3)	22.36	22.77	22.52	0.10
M2 6.0m x-comp cur (cm/s)	-30.22	30.06	0.27	14.47
M2 6.0m y-comp cur (cm/s)	-21.25	24.42	3.34	9.34
M2 2.5m x-comp cur (cm/s)	-26.24	30.34	1.00	14.34
M2 2.5m y-comp cur (cm/s)	-17.69	27.62	4.51	9.01
M2 1.0m temperature (° C)	28.48	29.40	28.97	0.23
M2 1.0m salinity (PSU)	35.26	36.08	35.64	0.22
M2 1.0m sigma-t (kg/m^3)	22.38	22.84	22.55	0.11
M2 1.0m pressure (dbar)	11.45	13.56	12.48	0.55

Parameter	Min	Max	Mean	Stan. Dev.
(b) 40-HOUR LOW-PASS (40hlp) DATA:				
FBIS1 barometric pressure (mb)	1012.43	1020.87	1017.23	2.37
FBIS1 air temperature (° C)	25.65	29.03	27.87	0.92
FBIS1 x-comp wind stress (Pa*10)	-0.33	0.02	-0.13	0.10
FBIS1 y-comp wind stress (Pa*10)	-0.25	0.57	0.14	0.23
SVLS1 barometric pressure (mb)	1012.64	1020.53	1016.94	2.16
SVLS1 air temperature (° C)	26.08	28.30	27.30	0.66
SVLS1 east wind stress (Pa*10)	-0.50	0.02	-0.20	0.15
SVLS1 north wind stress (Pa*10)	-0.41	0.40	0.04	0.20
M1 8.0m temperature (° C)	28.82	29.83	29.34	0.31
M1 8.0m salinity (PSU)	33.38	33.75	33.56	0.12
M1 8.0m sigma-t (kg/m^3)	20.72	21.17	20.87	0.13
M1 6.5m x-comp cur (cm/s)	4.47	13.22	7.47	1.74
M1 6.5m y-comp cur (cm/s)	-3.71	2.17	-0.64	1.44
M1 2.5m x-comp cur (cm/s)	2.47	10.14	5.36	1.56
M1 2.5m y-comp cur (cm/s)	-3.36	6.45	0.36	2.57
M1 1.0m temperature (° C)	28.82	29.82	29.32	0.31
M1 1.0m salinity (PSU)	33.37	33.85	33.58	0.15
M1 1.0m sigma-t (kg/m^3)	20.72	21.19	20.89	0.15
M1 1.0m pressure (dbar)	16.57	16.76	16.65	0.05
M2 7.0m temperature (° C)	28.65	29.25	28.97	0.20
M2 7.0m salinity (PSU)	35.29	35.89	35.59	0.18
M2 7.0m sigma-t (kg/m^3)	22.40	22.70	22.52	0.09
M2 6.0m x-comp current (cm/s)	-2.42	3.14	0.27	1.50
M2 6.0m y-comp current (cm/s)	-6.44	10.85	3.36	4.42
M2 2.5m x-comp current (cm/s)	-1.69	4.07	1.01	1.32
M2 2.5m y-comp current (cm/s)	-3.97	12.76	4.53	4.22
M2 1.0m temperature (° C)	28.64	29.26	28.98	0.22
M2 1.0m salinity (PSU)	35.31	36.01	35.64	0.22
M2 1.0m sigma-t (kg/m^3)	22.42	22.78	22.55	0.11
M2 1.0m pressure (dbar)	12.41	12.58	12.48	0.05

TABLE 5. First order statistics using 3hlp data for parameters measured for 2 tidal cycles each during the neap and spring tide of NED2. The station location and depth above bottom are designated for each sensor. All vectors with x and y components have the coordinate system rotated 50 degrees clockwise. (a) Neap tide data begin 26 August 1993 at 07 GMT and end 27 August 1993 at 08 GMT; (b) spring tide data begin 1 September 1993 at 00 GMT and end 2 September 1993 at 02 GMT.

Parameter	Min	Max	Mean	Stan. Dev.
(a) Neap Tide 3-HOUR LOW-PASS Data:				
FBIS1 barometric pressure (mb)	1018.92	1021.89	1020.30	0.85
FBIS1 air temperature (° C)	26.45	29.25	27.84	0.75
FBIS1 east wind stress (Pa*10)	-0.35	0.00	-0.12	0.08
FBIS1 north wind stress (Pa*10)	-0.24	0.14	-0.06	0.11
M1 8.0m temperature (° C)	28.47	29.54	29.02	0.28
M1 8.0m salinity (PSU)	32.36	34.07	33.51	0.55
M1 8.0m sigma-t (kg/m^3)	0.02	21.54	20.94	0.47
M1 6.5m x-comp current (cm/s)	-71.25	102.02	3.65	67.33
M1 6.5m y-comp current (cm/s)	-27.54	21.08	-1.05	16.75
M1 2.5m x-comp current (cm/s)	-69.15	82.02	2.25	54.71
M1 2.5m y-comp current (cm/s)	-18.80	16.84	-1.10	12.37
M1 1.0m temperature (° C)	28.46	29.44	28.99	0.27
M1 1.0m salinity (PSU)	32.36	34.06	33.49	0.52
M1 1.0m sigma-t (kg/m^3)	20.04	21.54	20.94	0.45
M1 1.0m pressure (dbar)	15.80	17.49	16.67	0.58
M2 7.0m temperature (° C)	28.48	28.82	28.66	0.11
M2 7.0m salinity (PSU)	35.24	35.38	35.32	0.05
M2 7.0m sigma-t (kg/m^3)	22.39	22.46	22.42	0.02
M2 6.0m x-comp cur (cm/s)	-22.03	23.81	2.54	13.26
M2 6.0m y-comp cur (cm/s)	-9.22	9.27	2.22	6.02
M2 2.5m x-comp cur (cm/s)	-22.09	24.25	3.86	13.20
M2 2.5m y-comp cur (cm/s)	-11.68	10.54	1.60	6.52
M2 1.0m temperature (° C)	28.48	28.81	28.65	0.10
M2 1.0m salinity (PSU)	35.26	35.40	35.33	0.04
M2 1.0m sigma-t (kg/m^3)	22.41	22.48	22.43	0.02
M2 1.0m pressure (dbar)	11.65	13.30	12.49	0.56

Parameter	Min	Max	Mean	Stan. Dev.
(b) Spring Tide 3-HOUR LOW-PASS Data:				
FBIS1 barometric pressure (mb)	1013.34	1018.50	1016.55	1.44
FBIS1 air temperature (° C)	27.62	30.23	28.77	0.87
FBIS1 east wind stress (Pa*10)	-0.25	0.06	-0.08	0.09
FBIS1 north wind stress (Pa*10)	0.11	0.66	0.34	0.16
M1 8.0m temperature (° C)	29.22	30.28	29.68	0.30
M1 8.0m salinity (PSU)	32.68	34.17	33.55	0.48
M1 8.0m sigma-t (kg/m^3)	20.12	21.29	20.75	0.36
M1 6.5m x-comp current (cm/s)	-90.56	126.81	3.87	80.80
M1 6.5m y-comp current (cm/s)	-28.62	21.36	0.06	18.28
M1 2.5m x-comp current (cm/s)	-74.03	100.39	1.29	66.82
M1 2.5m y-comp current (cm/s)	-23.63	28.23	1.44	17.80
M1 1.0m temperature (° C)	29.13	0.30	29.67	0.34
M1 1.0m salinity (PSU)	32.66	34.15	33.57	0.47
M1 1.0m sigma-t (kg/m^3)	20.12	21.37	20.77	0.36
M1 1.0m pressure (dbar)	15.78	17.60	16.71	0.64
M2 7.0m temperature (° C)	28.91	29.22	29.05	0.08
M2 7.0m salinity (PSU)	35.52	35.68	35.58	0.05
M2 7.0m sigma-t (kg/m^3)	22.42	22.58	22.49	0.05
M2 6.0m x-comp cur (cm/s)	-28.62	23.14	-0.40	15.55
M2 6.0m y-comp cur (cm/s)	-10.34	16.51	4.89	8.52
M2 2.5m x-comp cur (cm/s)	-18.52	24.17	4.44	14.54
M2 2.5m y-comp cur (cm/s)	-12.48	16.24	3.08	8.73
M2 1.0m temperature (° C)	28.91	29.11	29.02	0.05
M2 1.0m salinity (PSU)	35.54	35.76	35.61	0.06
M2 1.0m sigma-t (kg/m^3)	22.45	22.63	22.52	0.05
M2 1.0m pressure (dbar)	11.66	13.39	12.55	0.62

TABLE 6. First order statistics during NED2 using 40hlp data for parameters measured for the calm period and the windy period as defined in the text. The station location and depth above bottom are designated for each sensor. All vectors with x and y components have the coordinate system rotated 50 degrees clockwise. (a) The calm period extended from 25 August 1993 18 hr GMT until 31 August 1993 at 06 hr GMT; (b) the windy period extended from 13 August 1993 06 hr GMT until 5 September 1993 06 hr GMT.

Parameter	Min	Max	Mean	Stan. Dev.
(a) 40-HOUR LOW-PASS (40hlp) Data:				
FBIS1 barometric pressure (mb)	1014.94	1020.59	1017.88	1.84
FBIS1 air temperature (° C)	27.06	28.28	27.79	0.38
FBIS1 east wind stress (Pa*10)	-0.25	0.04	-0.11	0.07
FBIS1 north wind stress (Pa*10)	-0.25	0.07	-0.05	0.09
M1 8.0m temperature (° C)	28.91	29.65	29.19	0.22
M1 8.0m salinity (PSU)	33.38	33.54	33.45	0.05
M1 8.0m sigma-t (kg/m^3)	20.72	21.00	20.84	0.08
M1 6.5m x-comp current (cm/s)	5.09	10.58	7.64	1.42
M1 6.5m y-comp current (cm/s)	-3.71	0.87	-1.44	1.32
M1 2.5m x-comp current (cm/s)	3.36	8.37	5.58	1.27
M1 2.5m y-comp current (cm/s)	-3.36	2.46	-0.78	1.73
M1 1.0m temperature (° C)	28.86	29.64	29.16	0.22
M1 1.0m salinity (PSU)	33.37	33.56	33.44	0.05
M1 1.0m sigma-t (kg/m^3)	20.72	21.03	20.85	0.09
M1 1.0m pressure (dbar)	16.58	16.76	16.63	0.05
M2 7.0m temperature (° C)	28.65	28.98	28.77	0.10
M2 7.0m salinity (PSU)	35.29	35.55	35.43	0.09
M2 7.0m sigma-t (kg/m^3)	22.40	22.52	22.47	0.04
M2 6.0m x-comp current (cm/s)	-2.42	0.60	-0.48	0.87
M2 6.0m y-comp current (cm/s)	-1.59	4.12	1.70	1.63
M2 2.5m x-comp current (cm/s)	-1.69	1.59	0.81	0.85
M2 2.5m y-comp current (cm/s)	-0.18	4.32	2.76	1.16
M2 1.0m temperature (° C)	28.64	28.96	28.76	0.09
M2 1.0m salinity (PSU)	35.31	35.56	35.45	0.09
M2 1.0m sigma-t (kg/m^3)	22.42	22.54	22.49	0.04
M2 1.0m pressure (dbar)	12.41	12.58	12.46	0.05

Parameter	Min	Max	Mean	Stan. Dev.
(b) 40-HOUR LOW-PASS (40hlp) DATA:				
FBIS1 barometric pressure (mb)	1012.43	1020.87	1017.12	2.80
FBIS1 air temperature (° C)	27.59	29.03	28.62	0.44
FBIS1 east wind stress (Pa*10)	-0.33	-0.01	-0.18	0.12
FBIS1 north wind stress (Pa*10)	0.01	0.57	0.38	0.13
M1 8.0m temperature (° C)	29.35	29.83	29.64	0.16
M1 8.0m salinity (PSU)	33.49	33.75	33.60	0.08
M1 8.0m sigma-t (kg/m^3)	20.72	21.01	20.80	0.10
M1 6.5m x-comp current (cm/s)	4.47	8.40	6.66	1.17
M1 6.5m y-comp current (cm/s)	-0.88	2.17	0.52	1.06
M1 2.5m x-comp current (cm/s)	3.91	6.27	4.95	0.93
M1 2.5m y-comp current (cm/s)	-1.04	6.45	2.02	2.58
M1 1.0m temperature (° C)	29.32	29.82	29.63	0.16
M1 1.0m salinity (PSU)	33.48	33.85	33.64	0.12
M1 1.0m sigma-t (kg/m^3)	20.72	21.09	20.83	0.13
M1 1.0m pressure (dbar)	16.59	16.72	16.67	0.04
M2 7.0m temperature (° C)	28.98	29.25	29.14	0.10
M2 7.0m salinity (PSU)	35.52	35.83	35.64	0.08
M2 7.0m sigma-t (kg/m^3)	22.46	22.62	22.50	0.04
M2 6.0m x-comp current (cm/s)	-2.42	3.13	0.98	1.72
M2 6.0m y-comp current (cm/s)	-1.59	10.85	5.98	4.29
M2 2.5m x-comp current (cm/s)	-1.69	4.07	1.23	1.84
M2 2.5m y-comp current (cm/s)	-0.44	12.58	6.86	4.29
M2 1.0m temperature (° C)	28.96	29.26	29.14	0.11
M2 1.0m salinity (PSU)	35.53	35.95	35.69	0.11
M2 1.0m sigma-t (kg/m^3)	22.47	22.70	22.54	0.05
M2 1.0m pressure (dbar)	12.44	12.55	12.51	0.04

TABLE 7. Estimates of horizontal temperature and salinity gradients at M1 and M2 based on the one-dimensional conservation model described in the text. Data from the "TOP" sensors of SEACATs and S-4 current meters were used which represents the approximate middle of the water column. Units are km, deg C and psu for distance, temperature and salinity respectively. (a) NED2; (b) NED1 (for comparison).

	M1 (Inlet)		M2 (Offshore)	
	Neap	Spring	Neap	Spring
(a) NED2				
T(mean)	29.02	29.68	28.66	29.05
T(rms)	0.33	0.36	0.13	0.10
S(mean)	33.51	33.55	35.32	35.58
S(rms)	0.65	0.57	0.06	0.06
u(mean)	3.65	3.87	2.54	-0.40
u(rms)	80	96	16	18
$\partial T/\partial x$	0.037	0.033	0.072	0.049
$\partial S/\partial x$	0.072	0.053	0.033	0.030
(b) NED1				
T(mean)	23.42	22.64	20.54	21.55
T(rms)	0.65	0.68	0.18	0.10
S(mean)	30.51	31.79	33.84	34.46
S(rms)	1.52	1.62	0.25	0.04
u(mean)	-2.2	7.3	2.1	-1.4
u(rms)	86	108	20	21
$\partial T/\partial x$	0.067	0.056	0.080	0.042
$\partial S/\partial x$	0.157	0.134	0.111	0.017

(a)

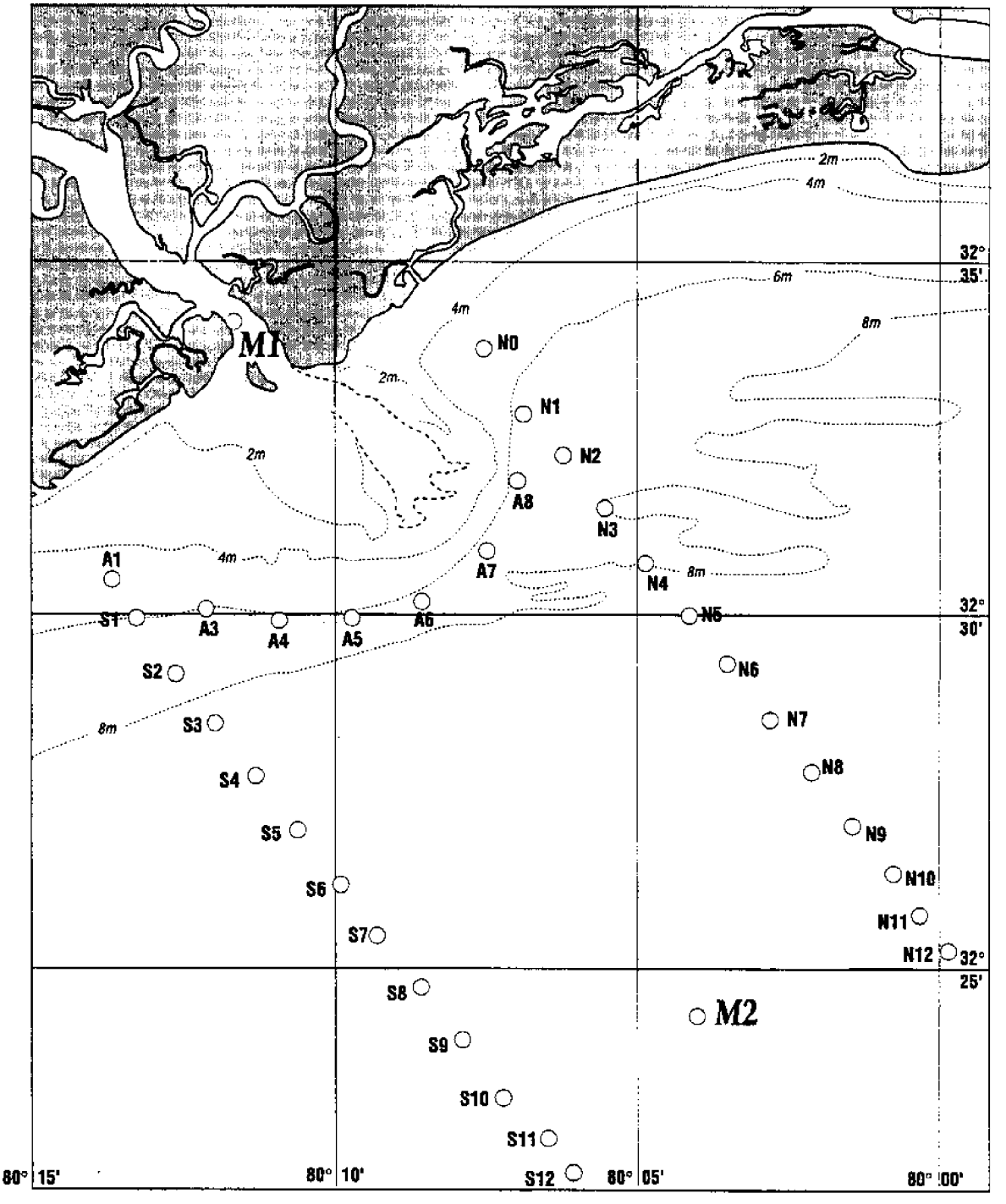

Fig. 1a. Location maps showing bathymetry and station locations for moorings and ship sampling. (a) Offshore domain covered by R/V BLUE FIN; (b) inlet domain covered primarily by R/V ANITA.

(b)

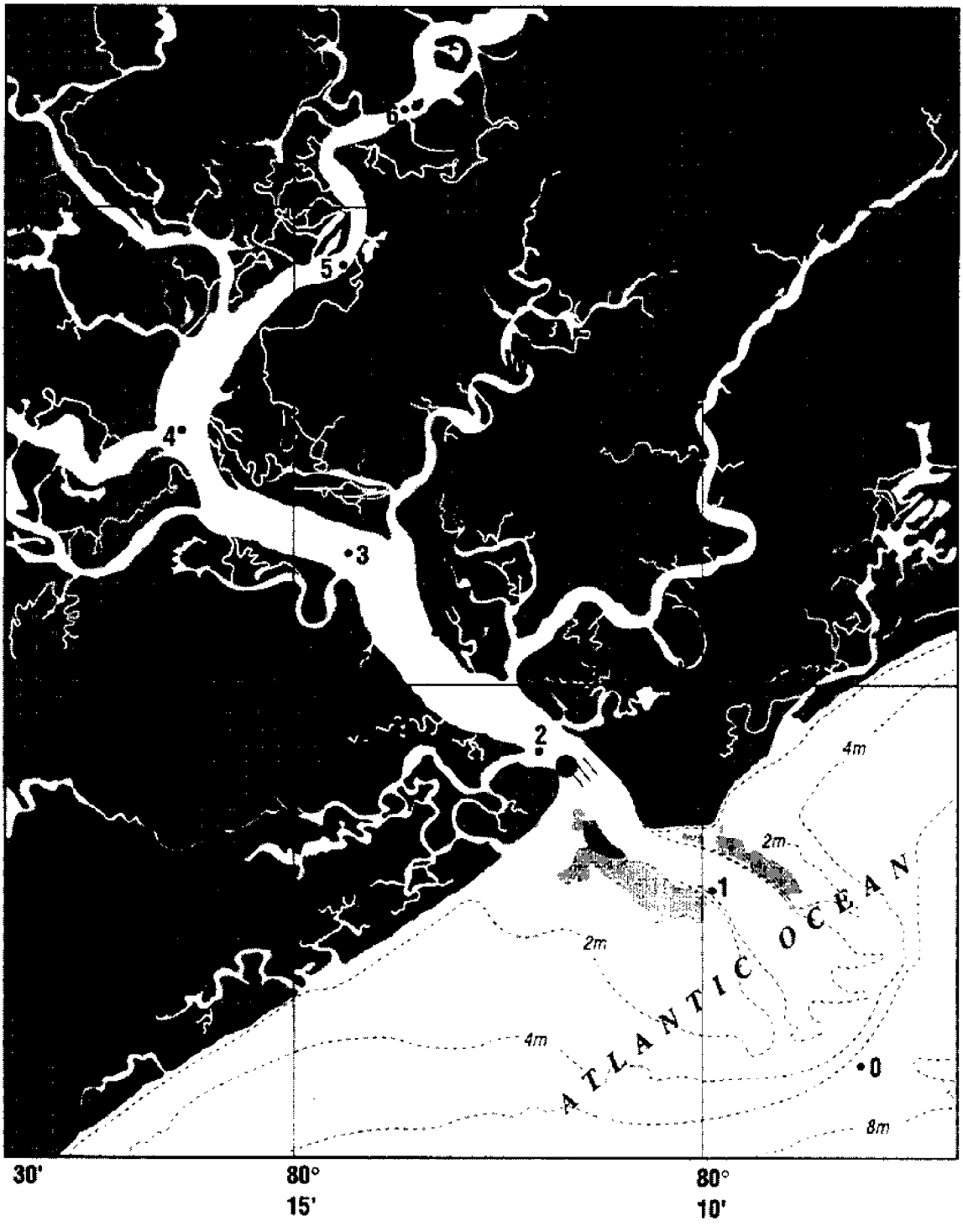

Fig. 1b. Location maps showing bathymetry and station locations for moorings and ship sampling. (a) Offshore domain covered by R/V BLUE FIN; (b) inlet domain covered primarily by R/V ANITA.

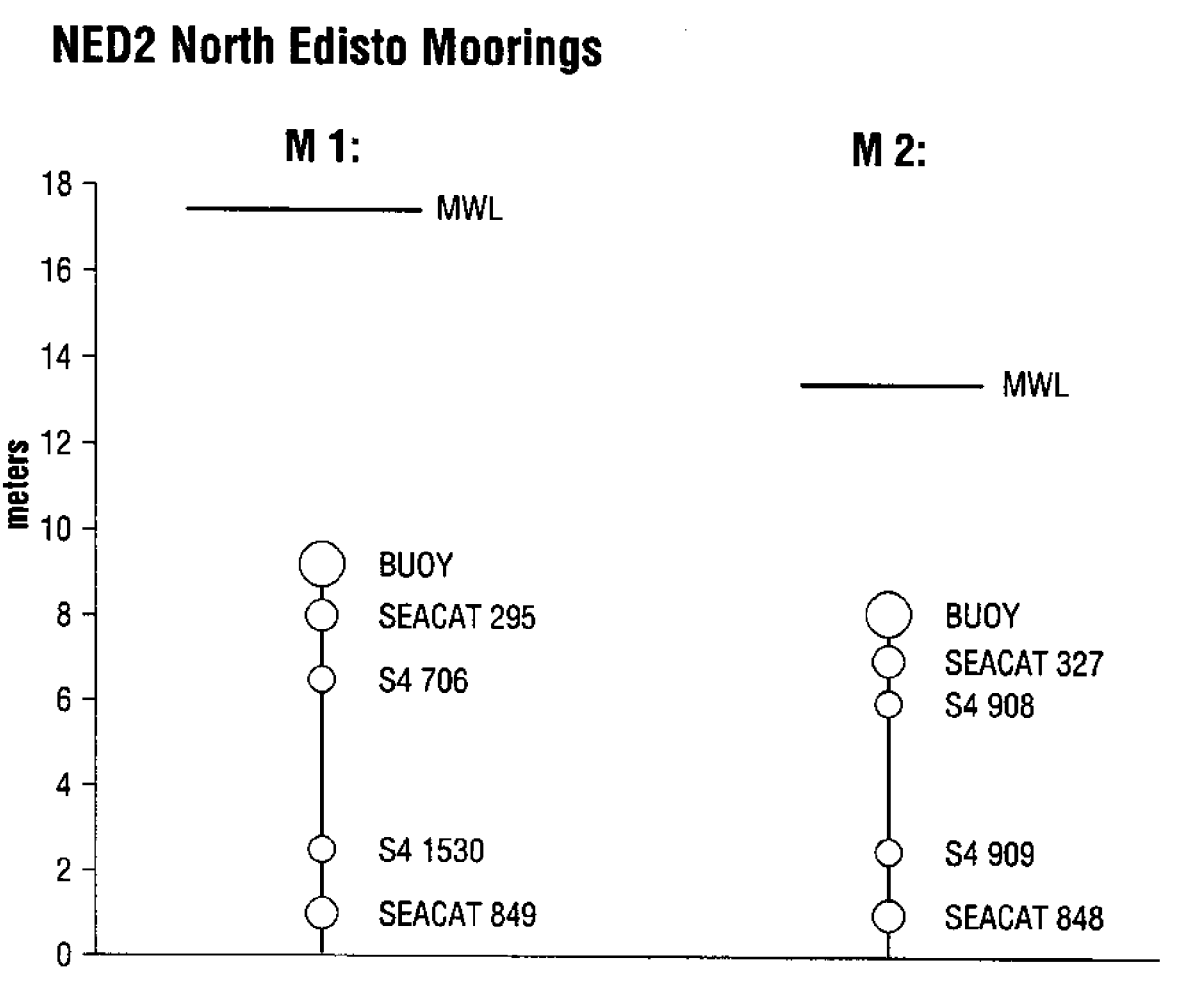

Fig. 2. Mooring design for stations M1 and M2 during NED2.

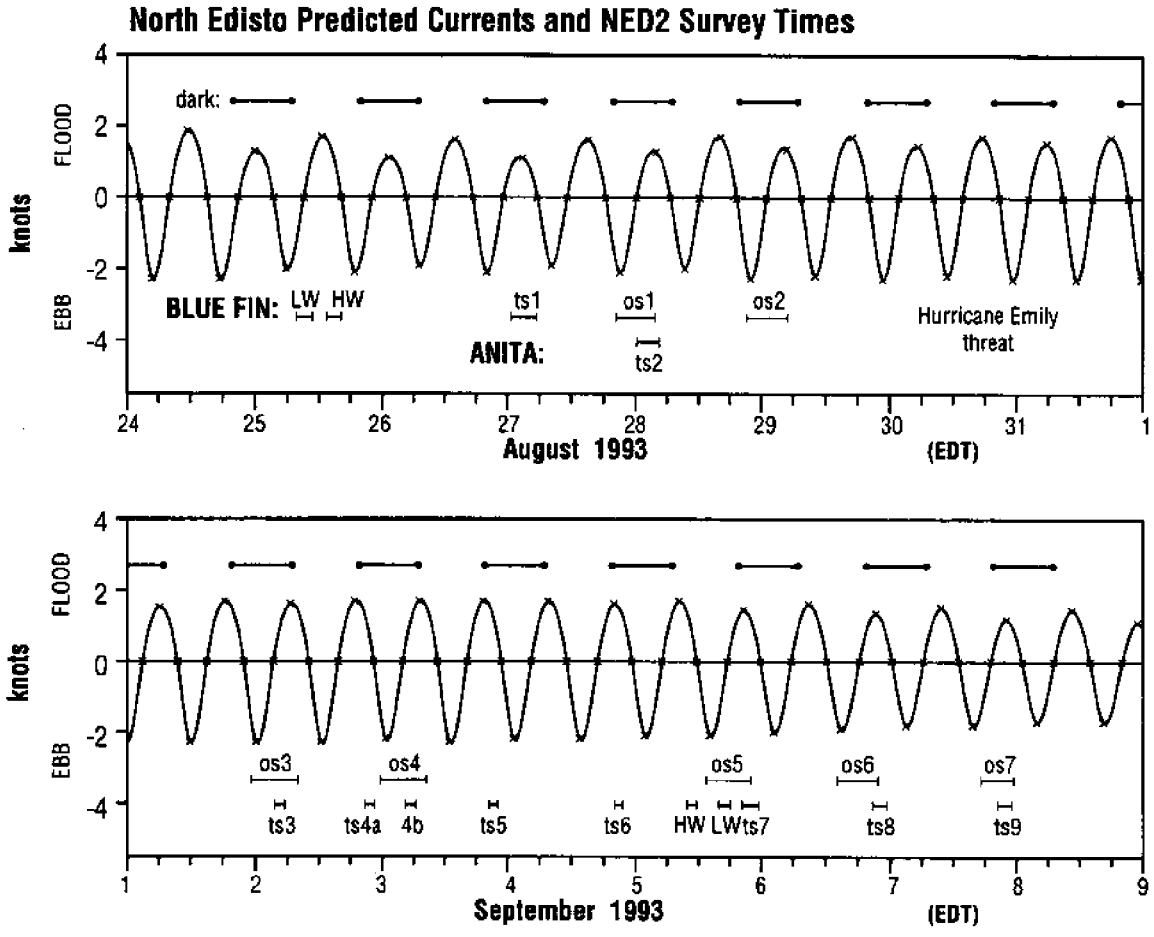

Fig. 3. Sampling times of offshore and inlet surveys in relation to cycles of tide and darkness. Predicted flood currents are positive and time is Eastern Daylight Savings Time.

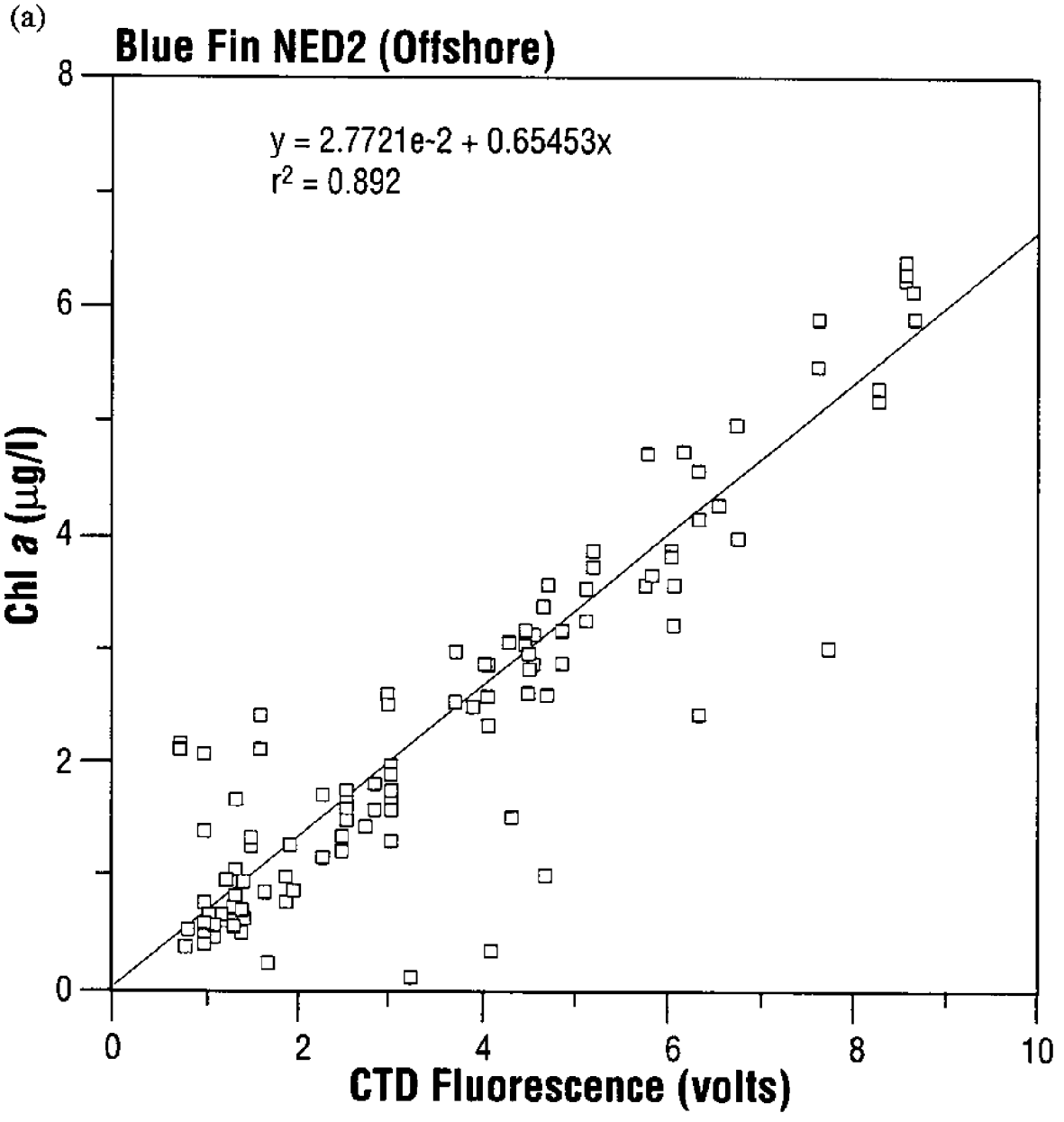

Fig. 4. Calibration curves of CTD fluorometer voltages versus extracted chlorophyll *a*. (a) R/V ANITA; (b) R/V BLUE FIN.

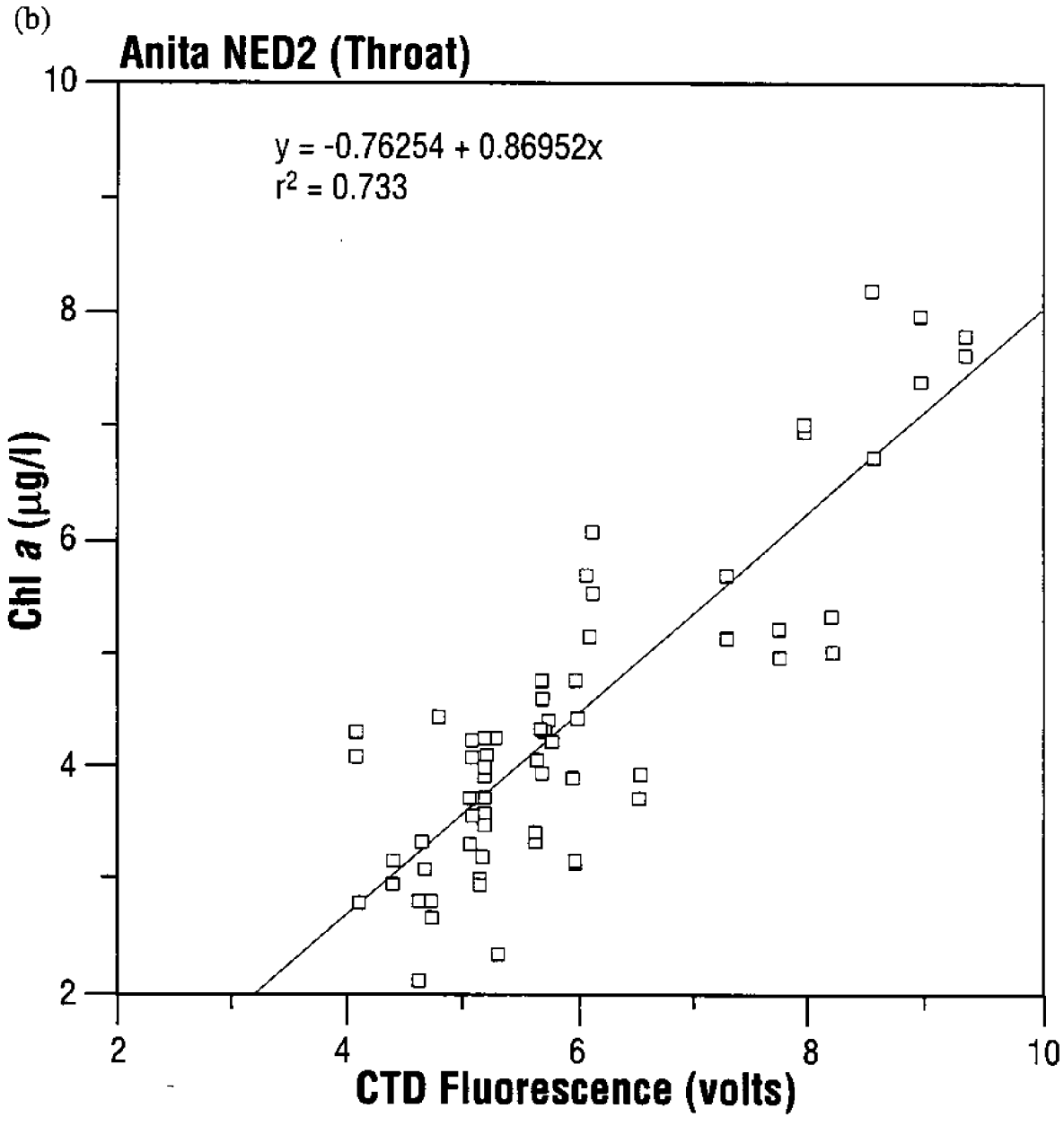

Fig. 4. Calibration curves of CTD fluorometer voltages versus extracted chlorophyll *a*. (a) R/V ANITA; (b) R/V BLUE FIN.

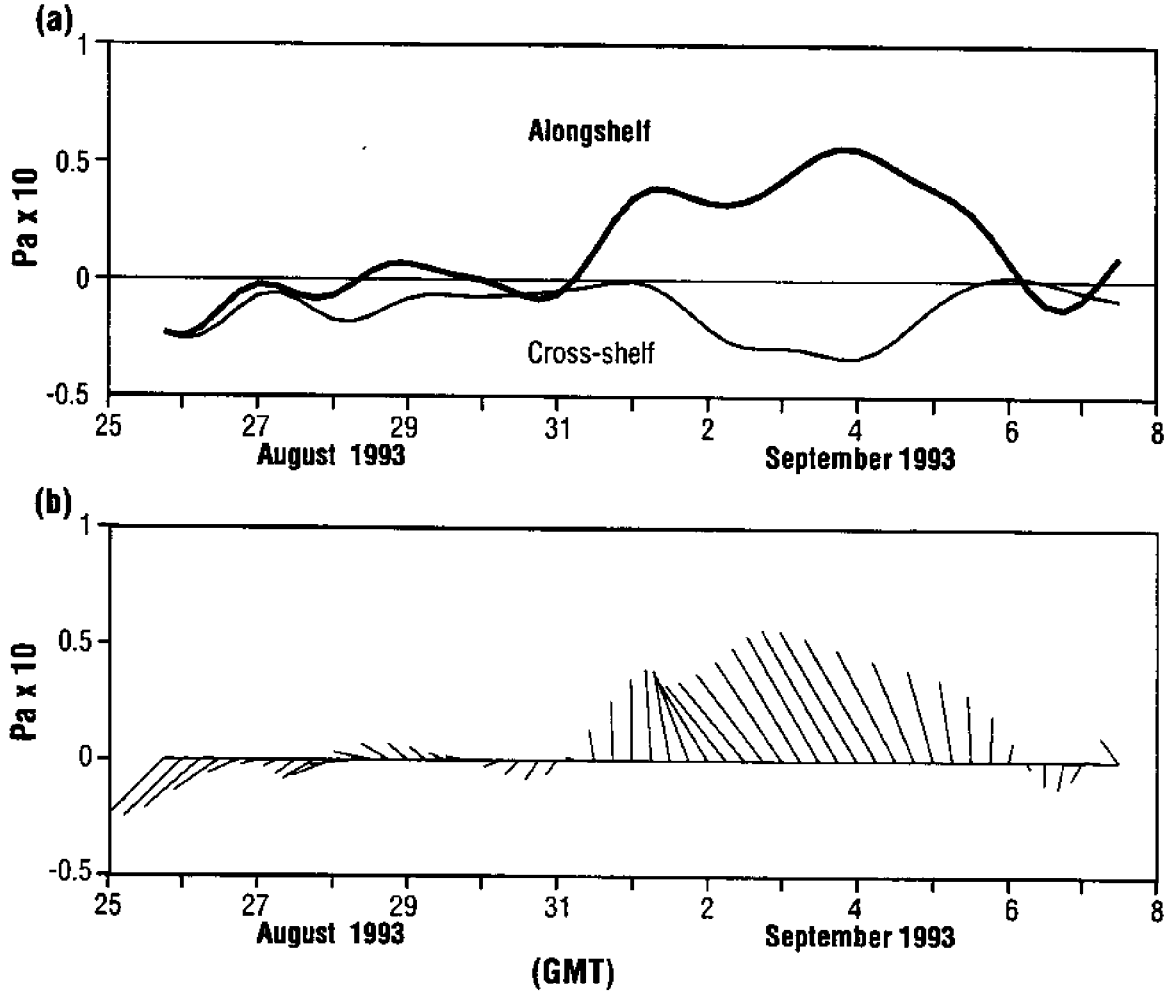

Fig. 5. Time series of rotated wind stress at FBIS1. Hourly data have been smoothed with a 40-hour low-pass filter and rotated 50 degrees counter-clockwise. (a) Alongshelf and cross-shelf components; (b) vector plot.

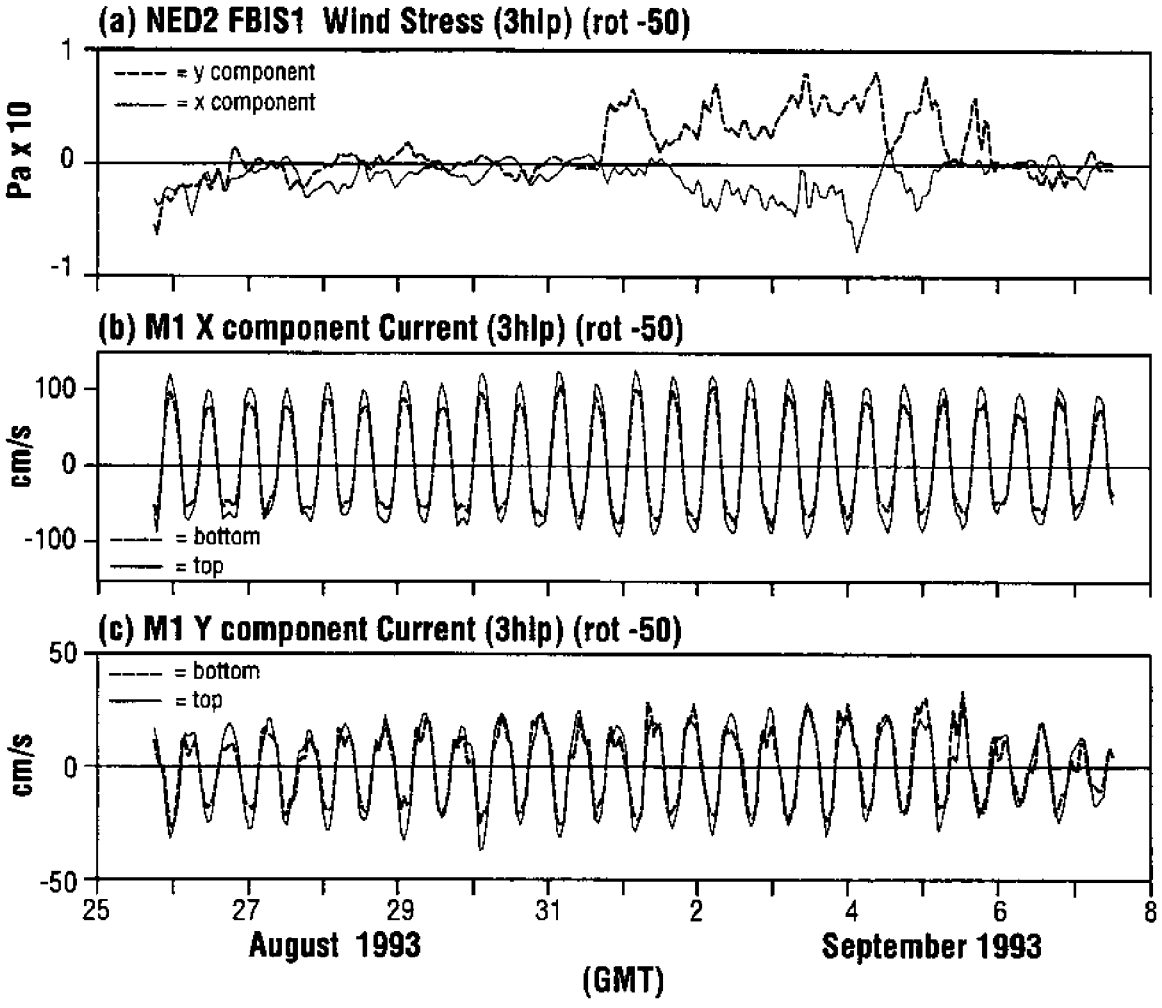

Fig. 6. Time series of 3hlp current data from M1. (a) Wind Stress components at FBIS1; (b) along-inlet current component (positive seaward); (c) cross-inlet current component (positive northeastward).

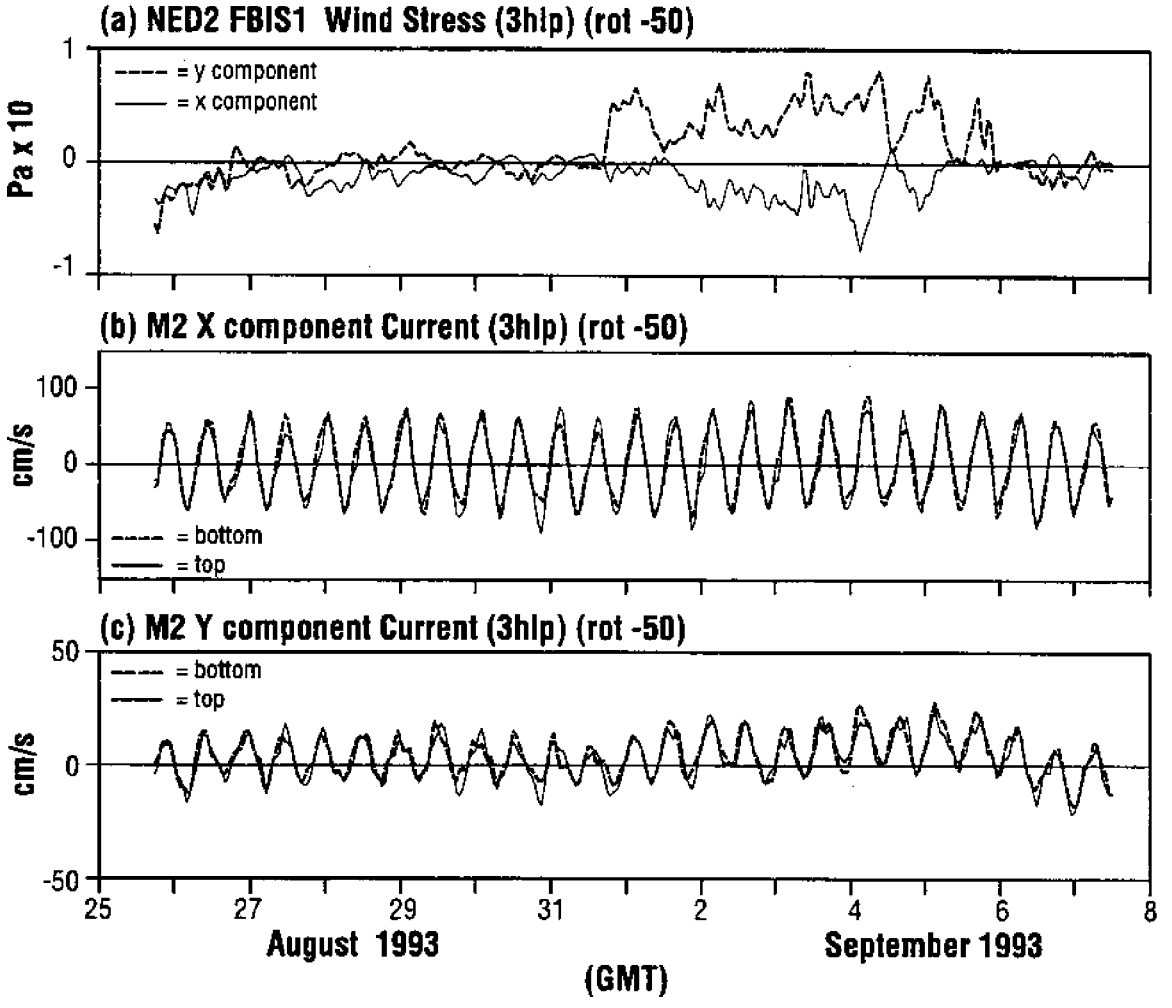

Fig. 7. Time series of 3hlp current data from M2. (a) Wind Stress components at FBIS1; (b) cross-shelf component (positive offshore); (c) alongshelf component (positive northeastward).

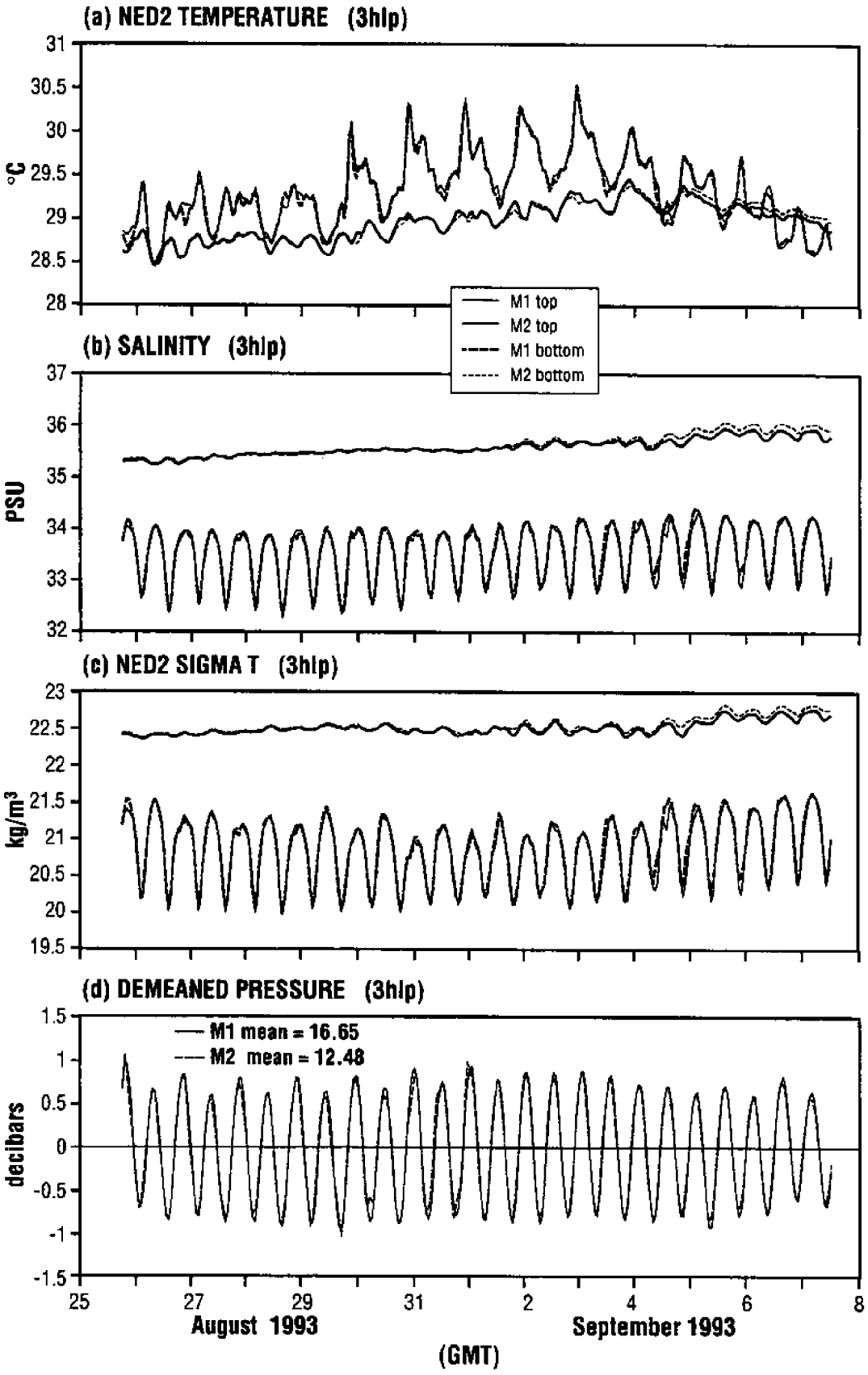

Fig. 8. Time series of 3hlp data from M1 and M2. Largest fluctuations occur at M1. Note that 2°C has been subtracted from temperature data for M2. (a) Temperature; (b) Salinity; (c) σ_t; (d) subsurface pressure.

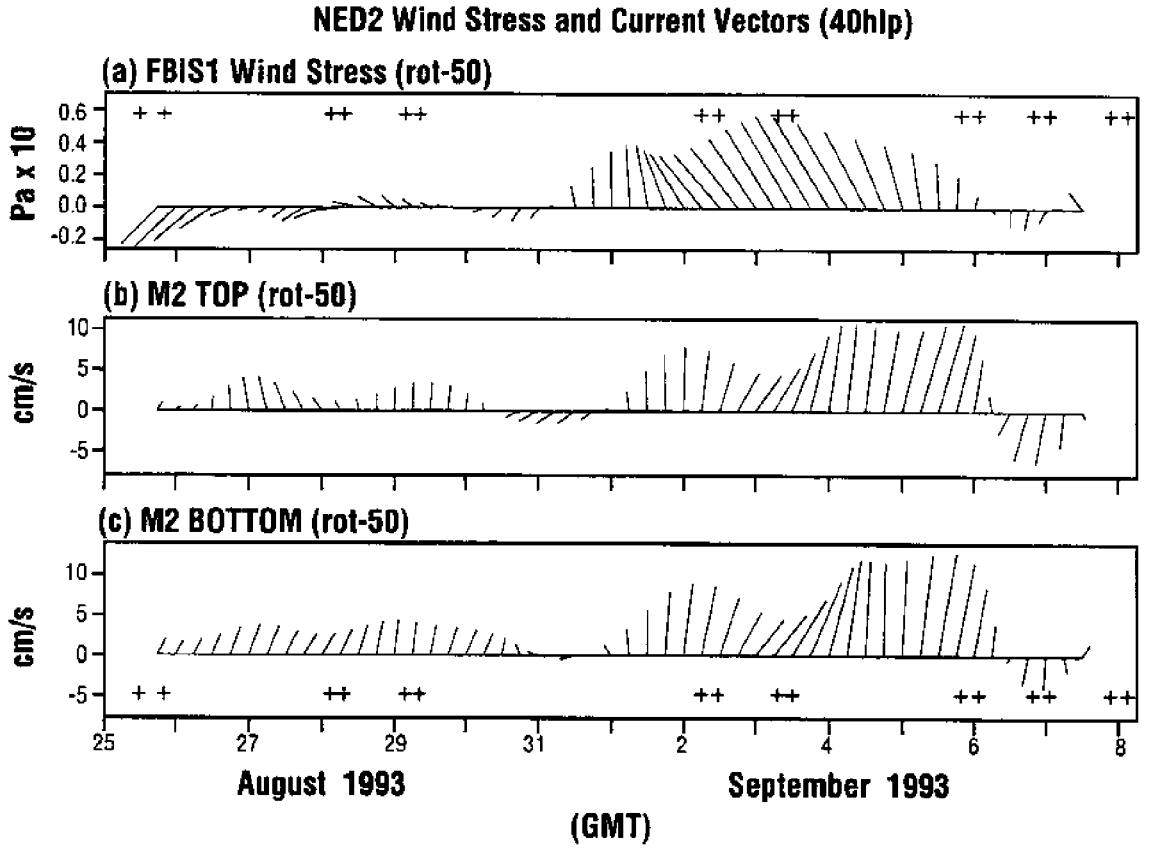

Fig. 9. Vector plots of 40hlp wind stress at FBIS1 and coastal currents at M2. Survey dates are denoted by crosses.

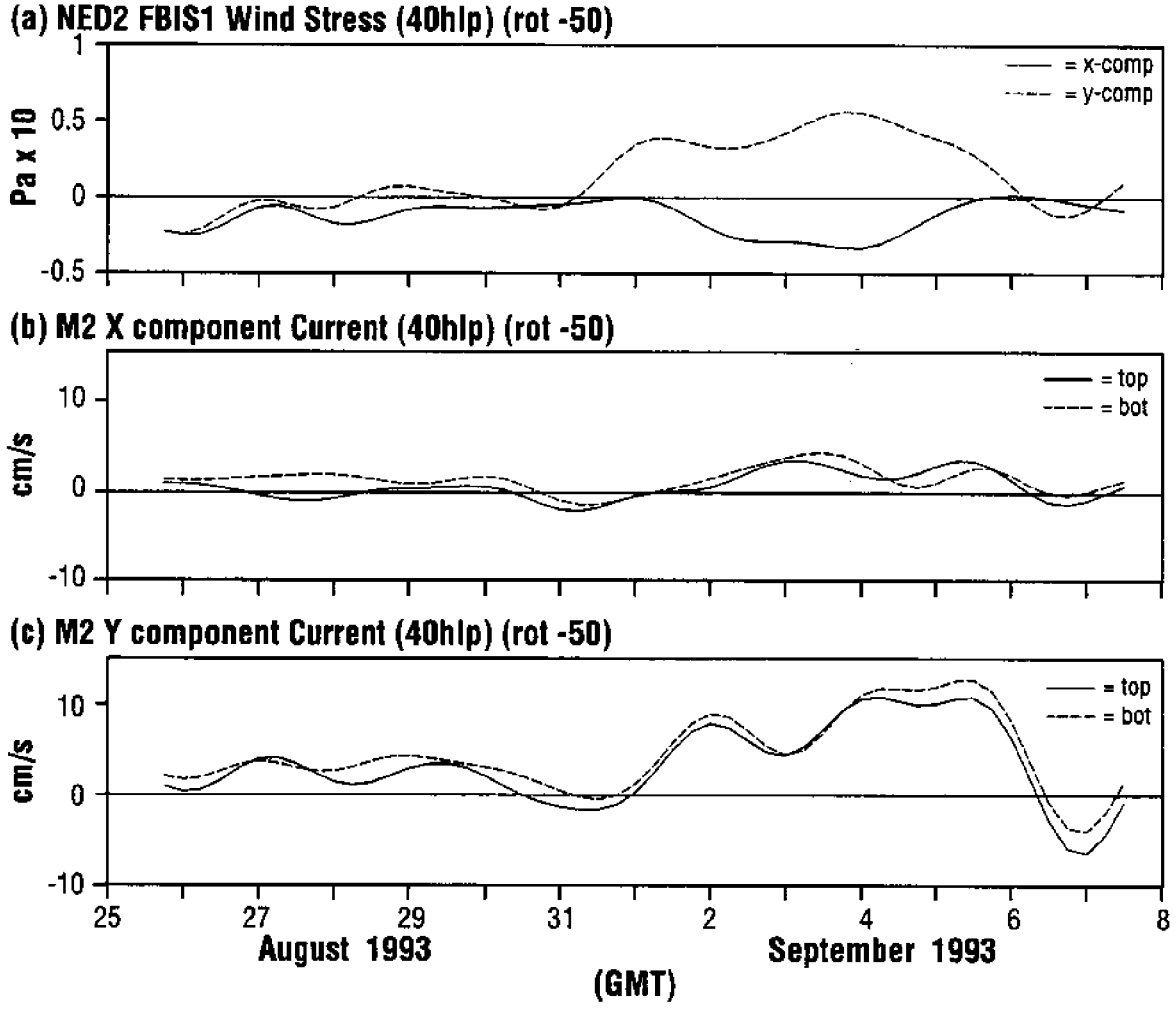

Fig. 10. Component plots of 40hlp wind stress at FBIS1 and coastal currents at M2.

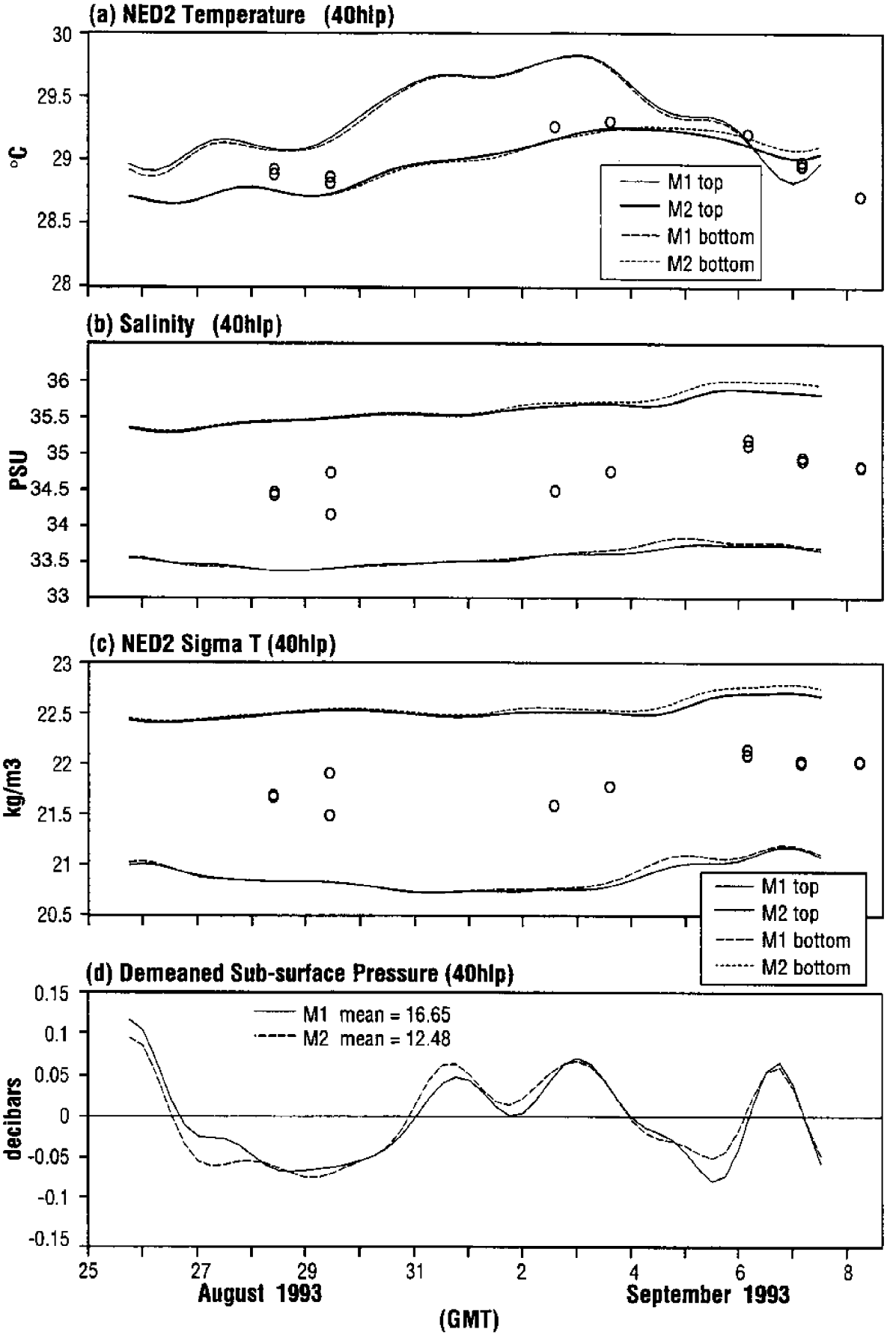

Fig. 11. Time series plots of 40hlp data from M1 and M2. (a) Temperature; (b) salinity; (c) σ_t; (d) subsurface pressure. Surface and bottom temperature and salinity (denoted by open circles) from the offshore surveys added for arc station A6.

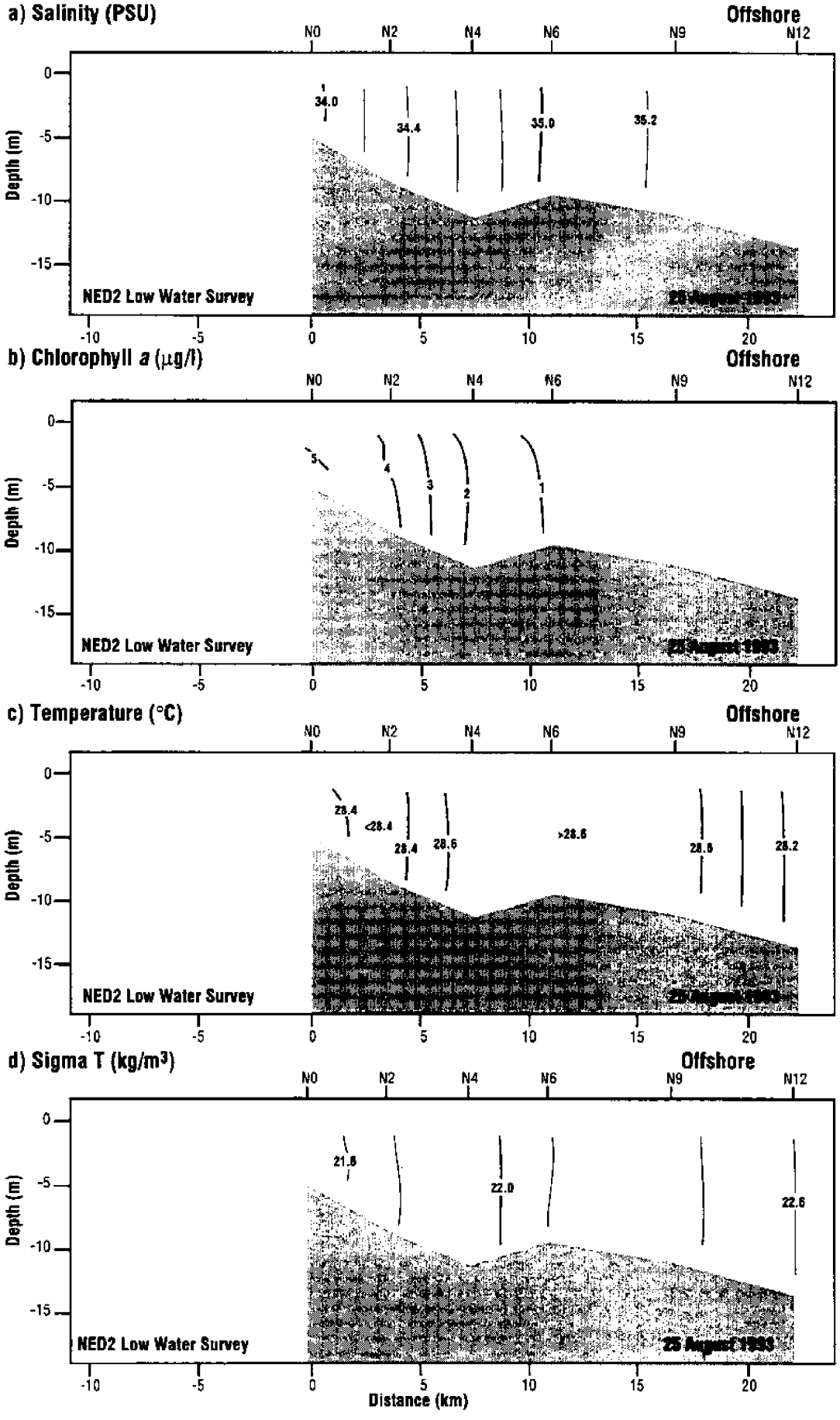

Fig. 12. Oceanographic survey at low water: 25 August 1993. (a) Salinity; (b) chlorophyll *a*; (c) temperature; (d) σ_t. See Figure 1 for station locations.

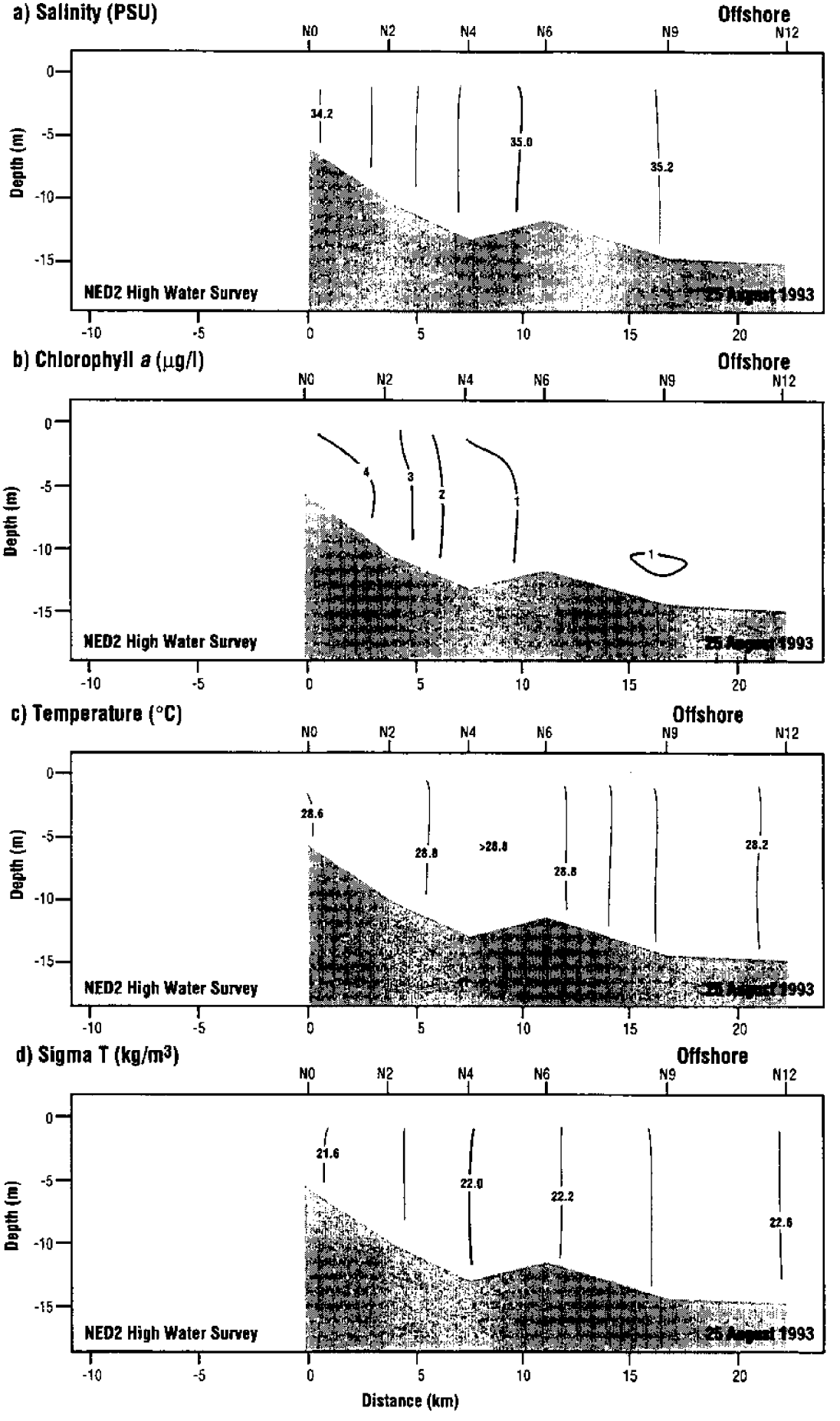

Fig. 13. Oceanographic survey at high water: 25 August 1993. (a) Salinity; (b) chlorophyll *a*; (c) temperature; (d) σ_t. See Figure 1 for station locations.

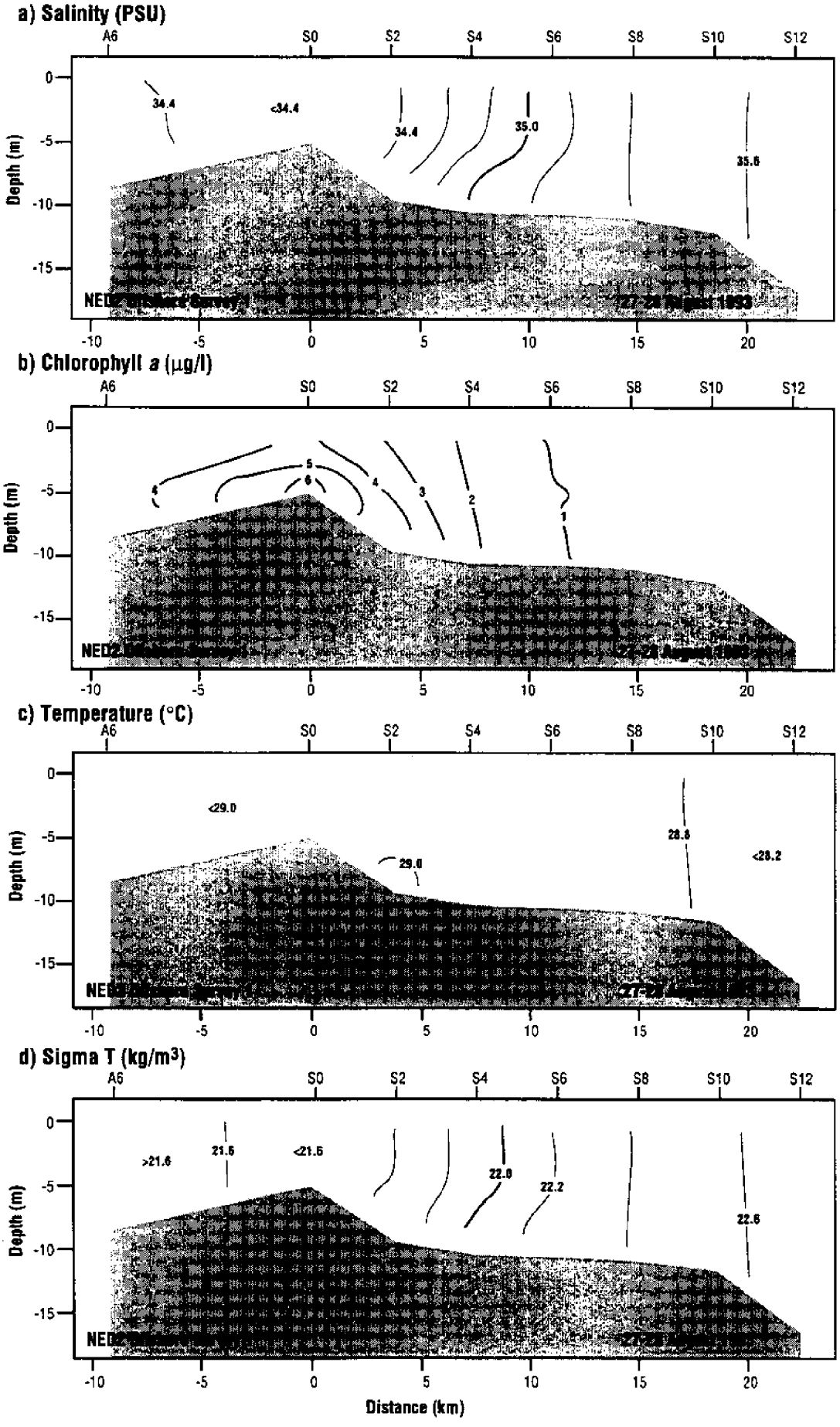

Fig. 14. Oceanographic and larval survey OS1: 27-28 August 1993. (a) Salinity; (b) chlorophyll *a*; (c) temperature; (d) σ_t. See Figure 1 for station locations.

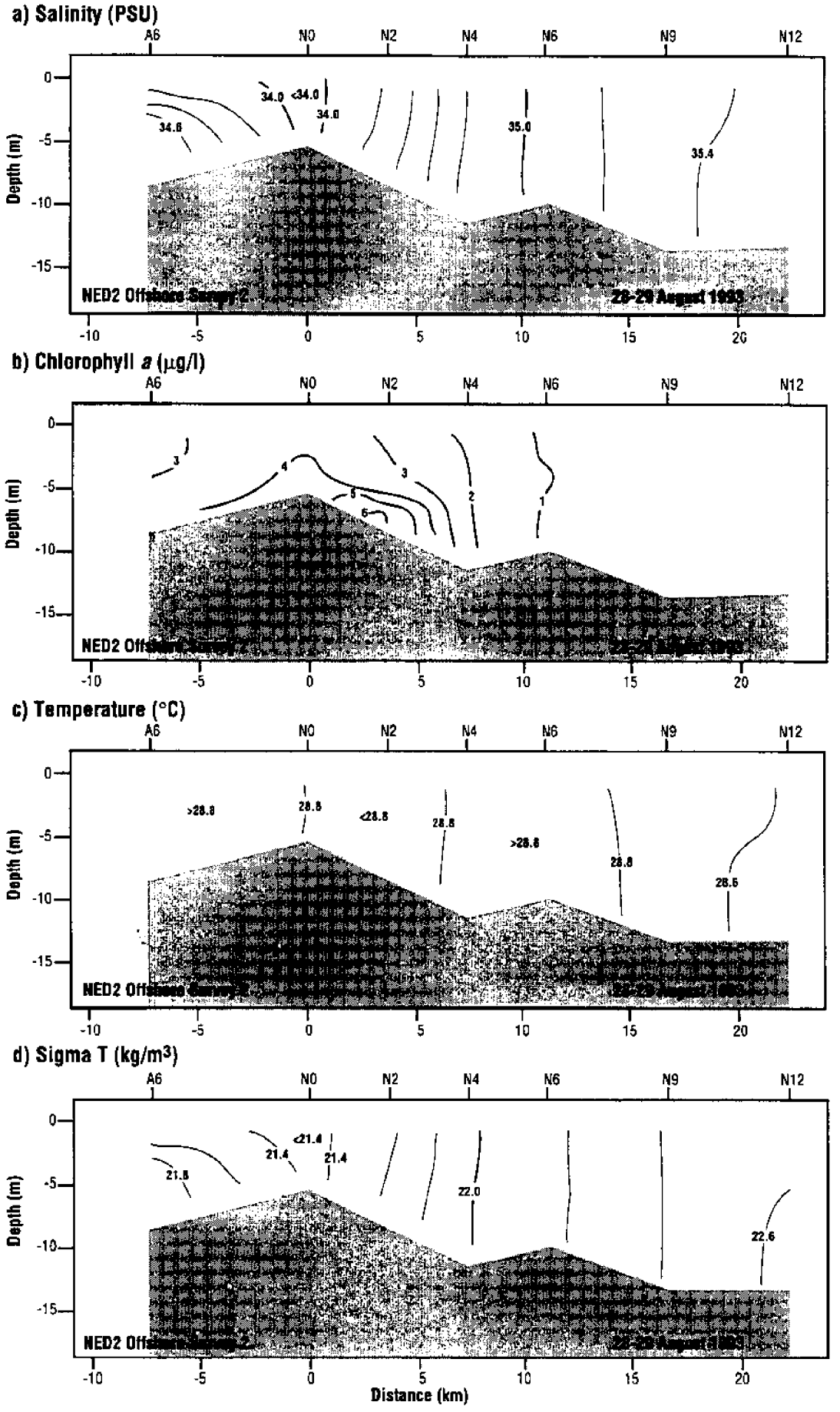

Fig. 15. Oceanographic and larval survey OS2: 28-29 August 1993. (a) Salinity; (b) chlorophyll *a*; (c) temperature; (d) σ_t. See Figure 1 for station locations.

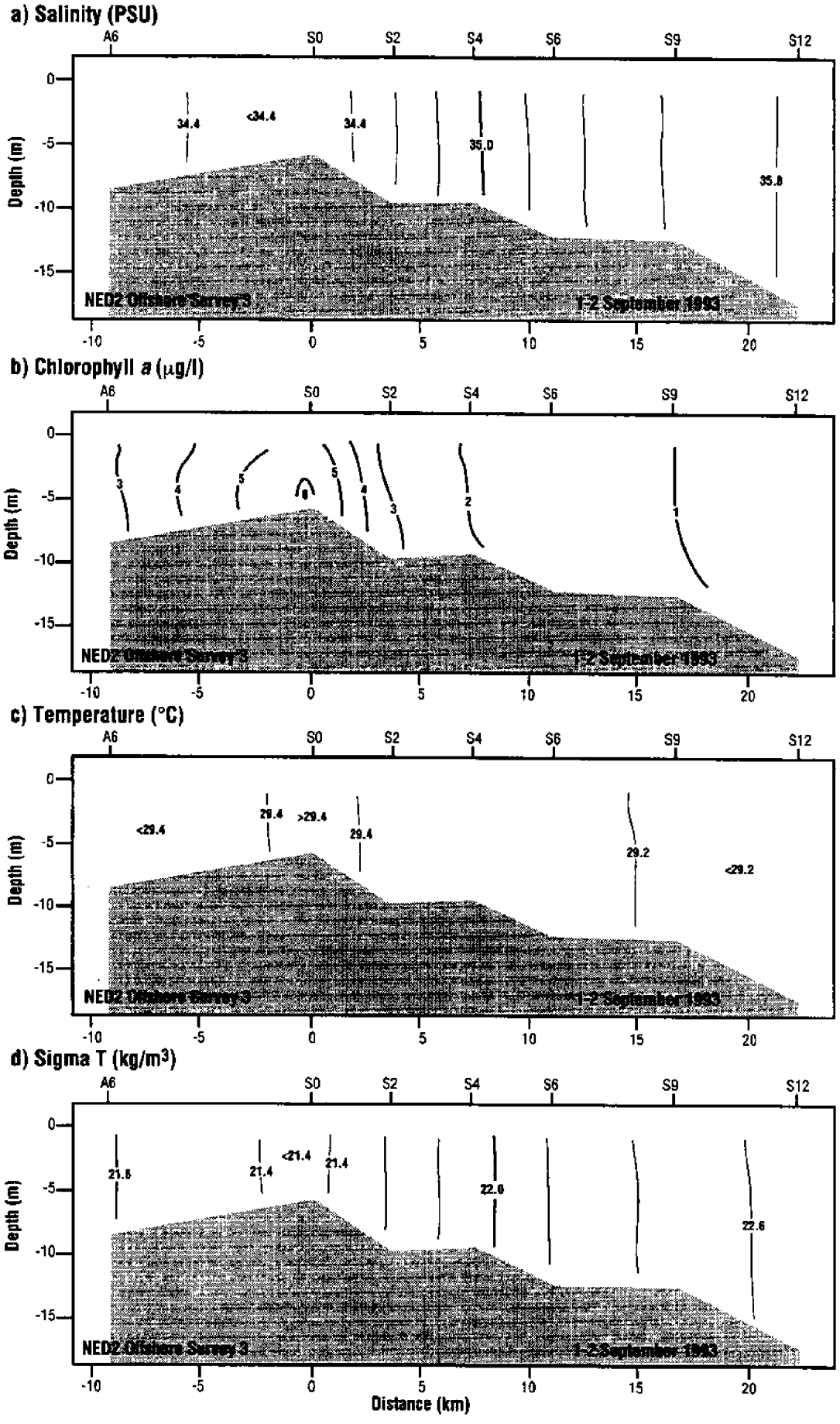

Fig. 16. Oceanographic and larval survey OS3: 1-2 September 1993. (a) Salinity; (b) chlorophyll *a*; (c) temperature; (d) σ_t. See Figure 1 for station locations.

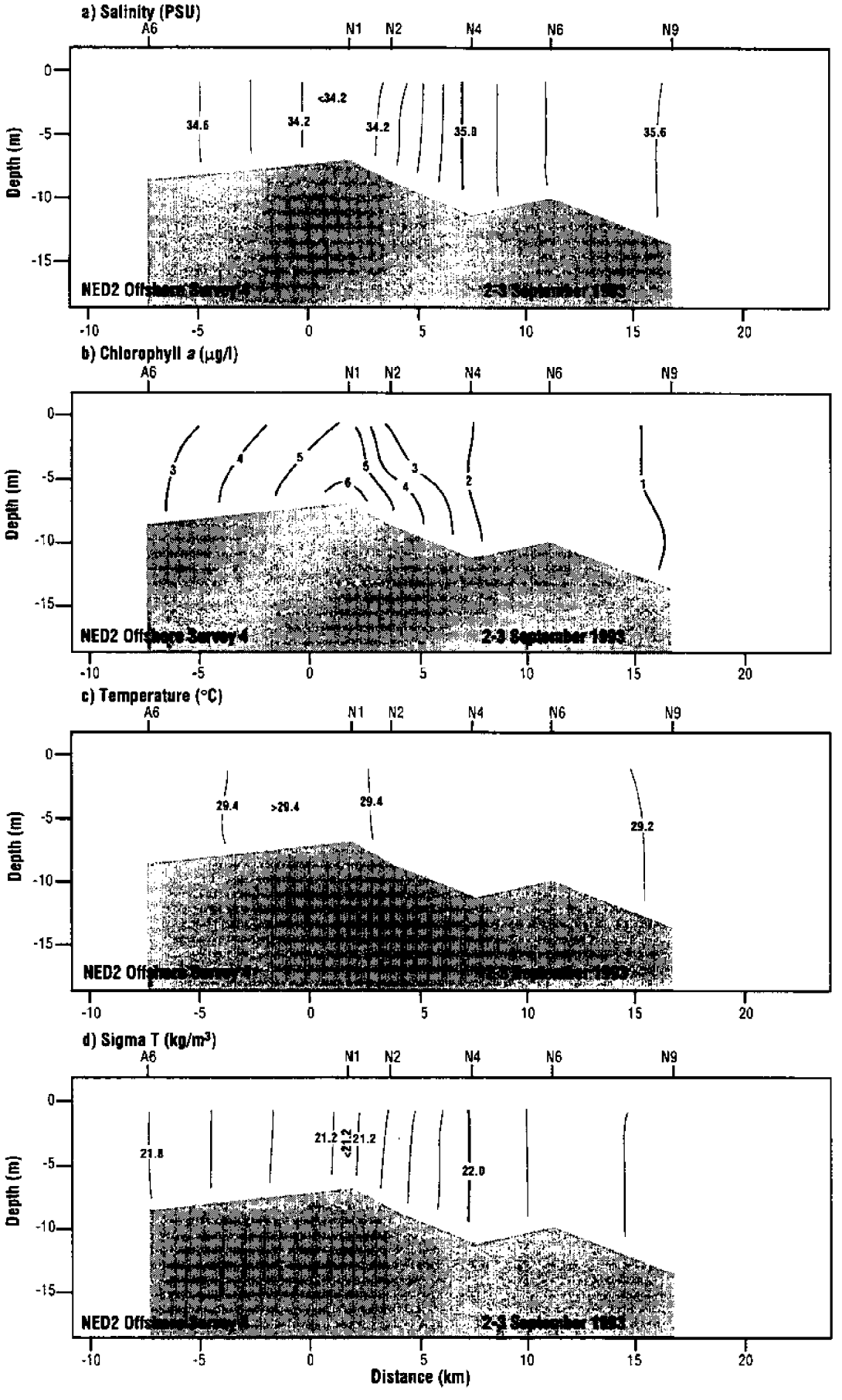

Fig. 17. Oceanographic and larval survey OS4: 2-3 September 1993. (a) Salinity; (b) chlorophyll *a*; (c) temperature; (d) σ_t. See Figure 1 for station locations.

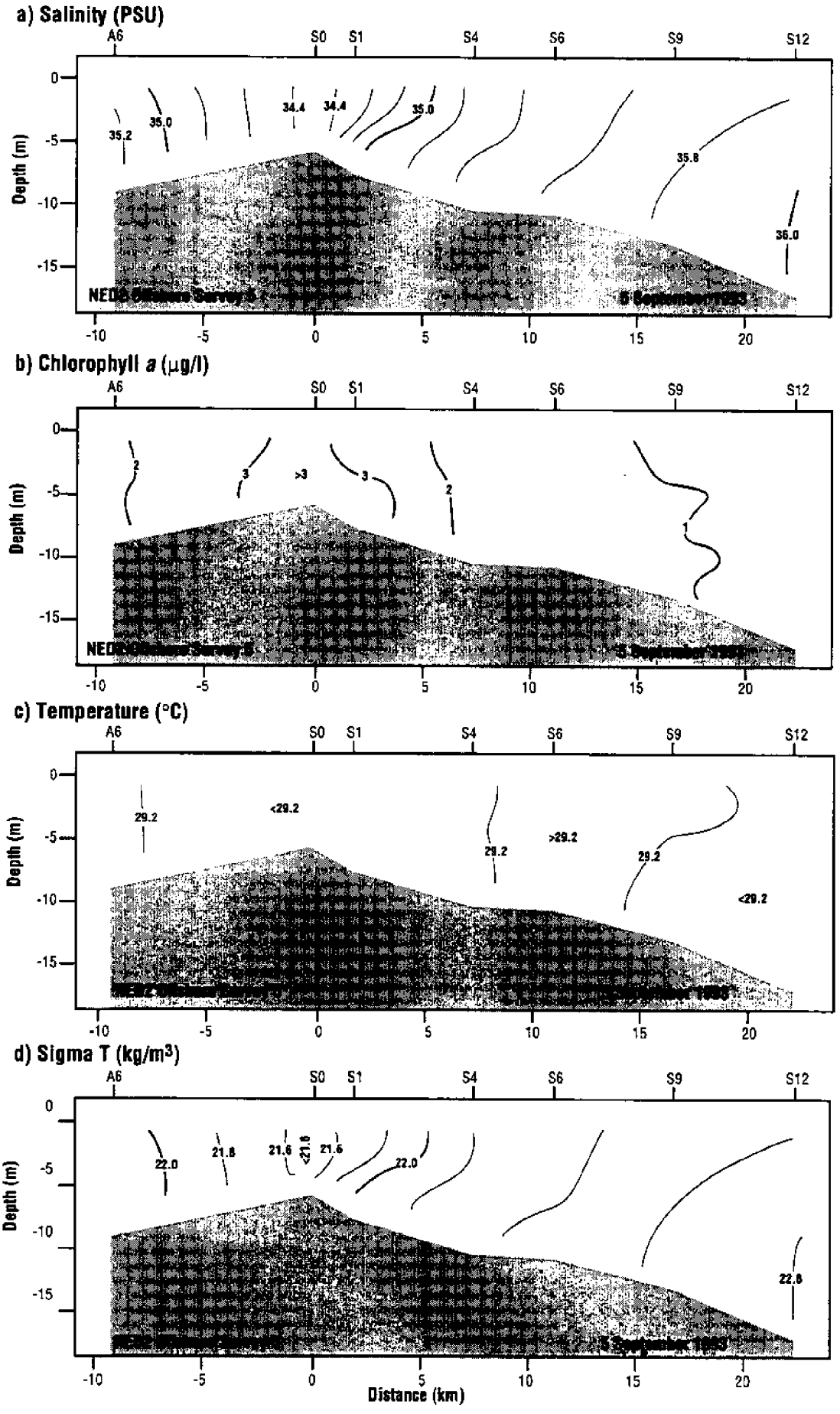

Fig. 18. Oceanographic and larval survey OS5: 5 September 1993. (a) Salinity; (b) chlorophyll *a*; (c) temperature; (d) σ_t. See Figure 1 for station locations.

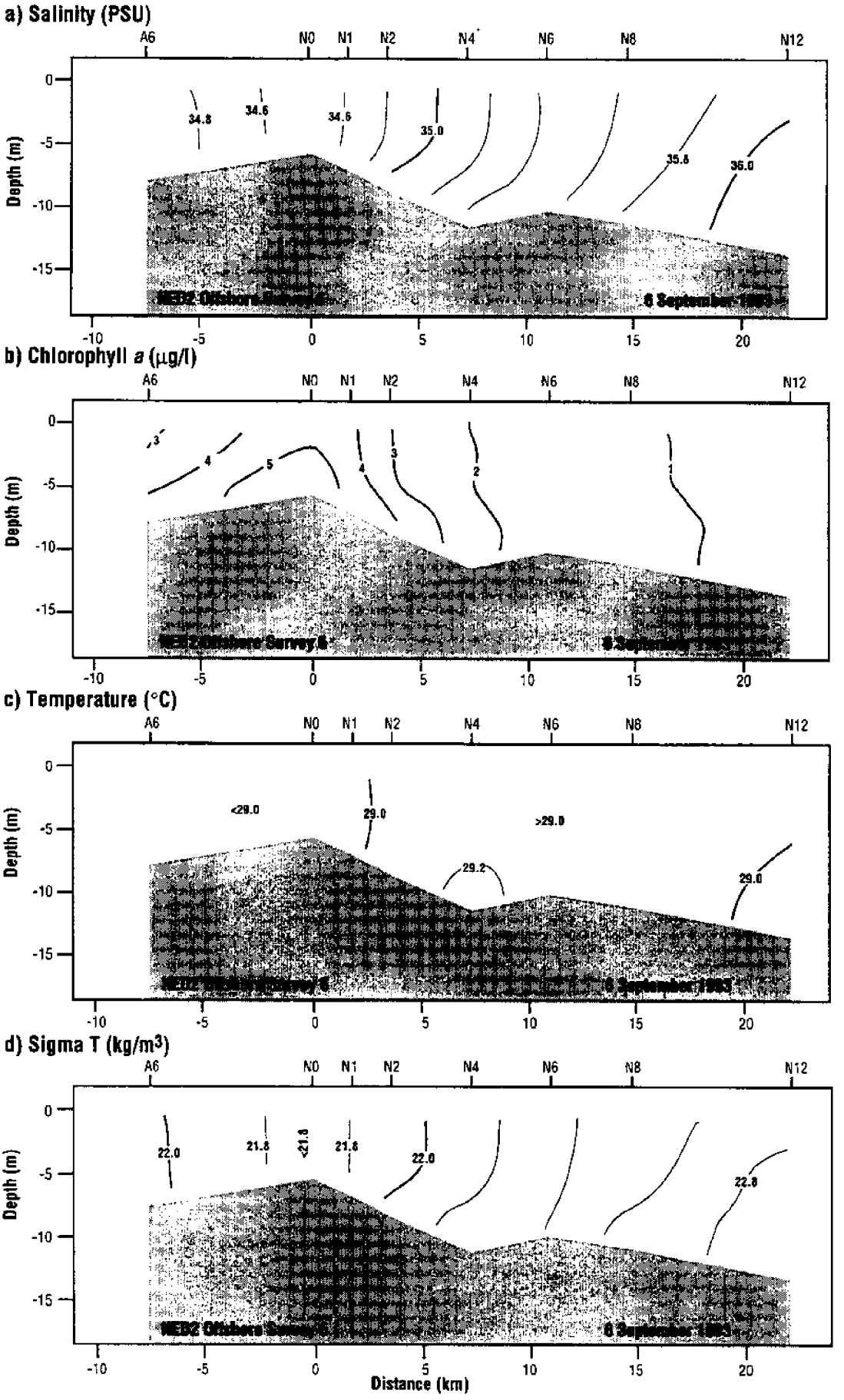

Fig. 19. Oceanographic and larval survey OS6: 6 September 1993. (a) Salinity; (b) chlorophyll *a*; (c) temperature; (d) σ_t. See Figure 1 for station locations.

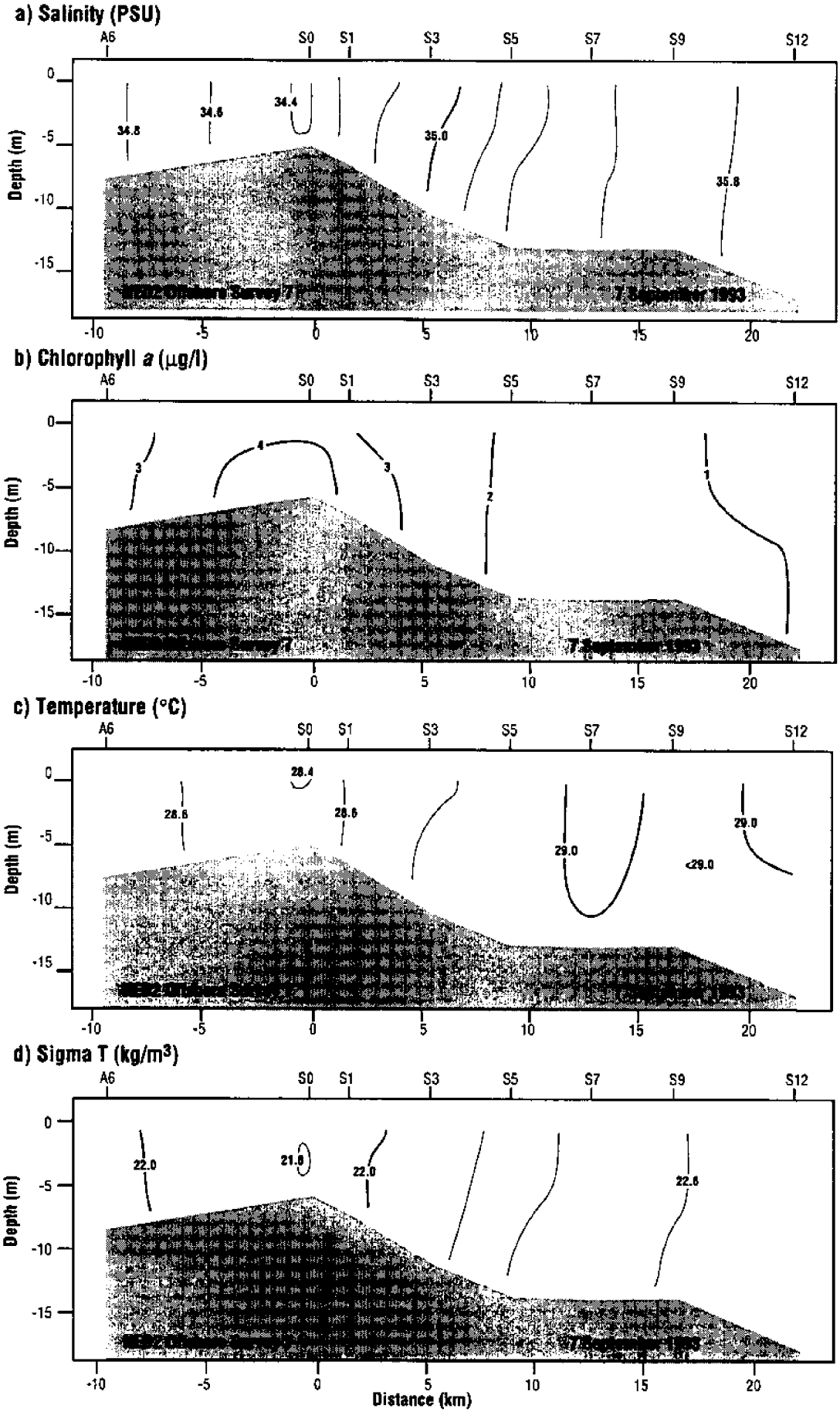

Fig. 20. Oceanographic and larval survey OS7: 7 September 1993. (a) Salinity; (b) chlorophyll *a*; (c) temperature; (d) σ_t. See Figure 1 for station locations.

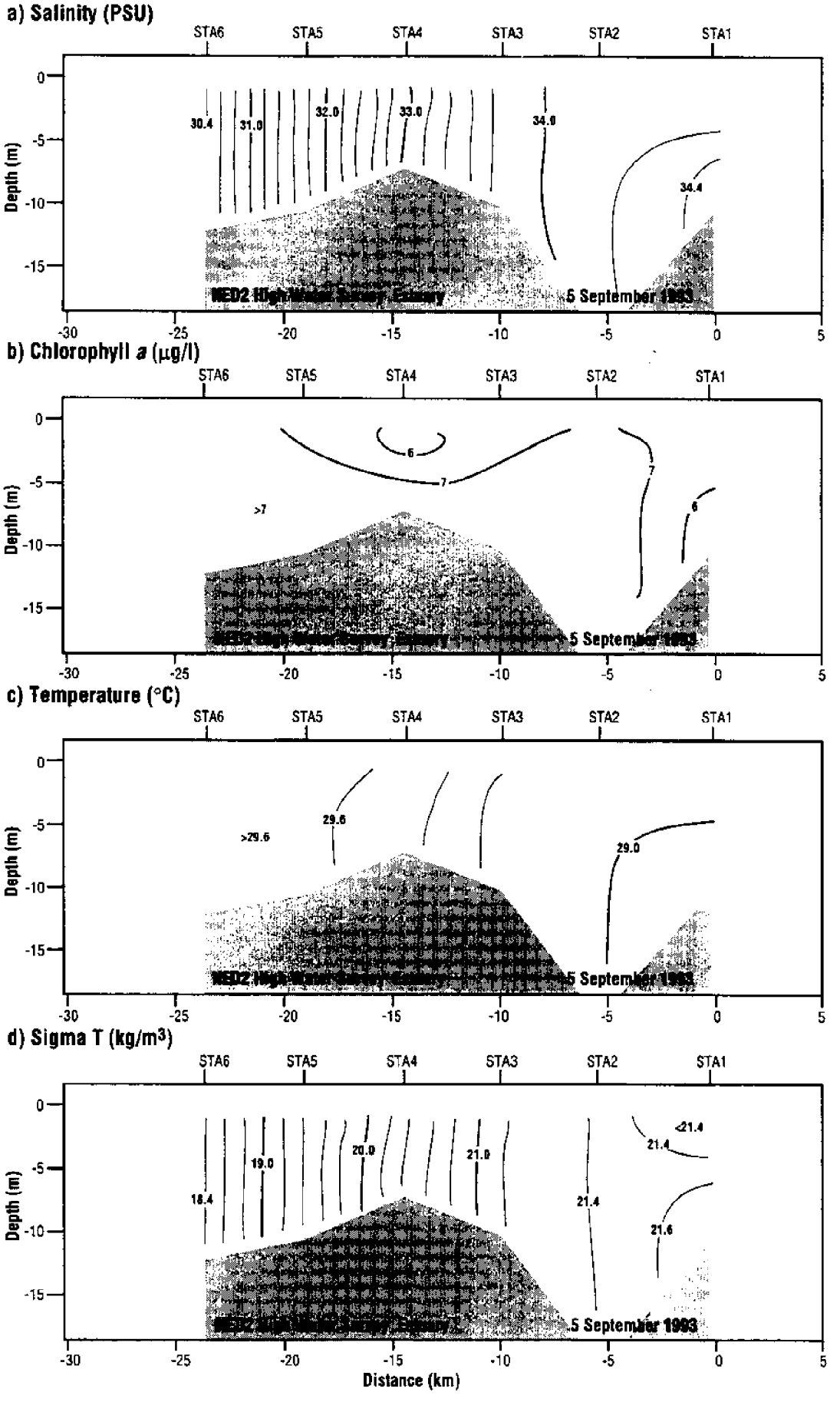

Fig. 21. Estuarine survey in the North Edisto River during high water on 5 September 1993. (a) Salinity; (b) chlorophyll *a*; (c) temperature; (d) σ_t. See Figure 1 for station locations.

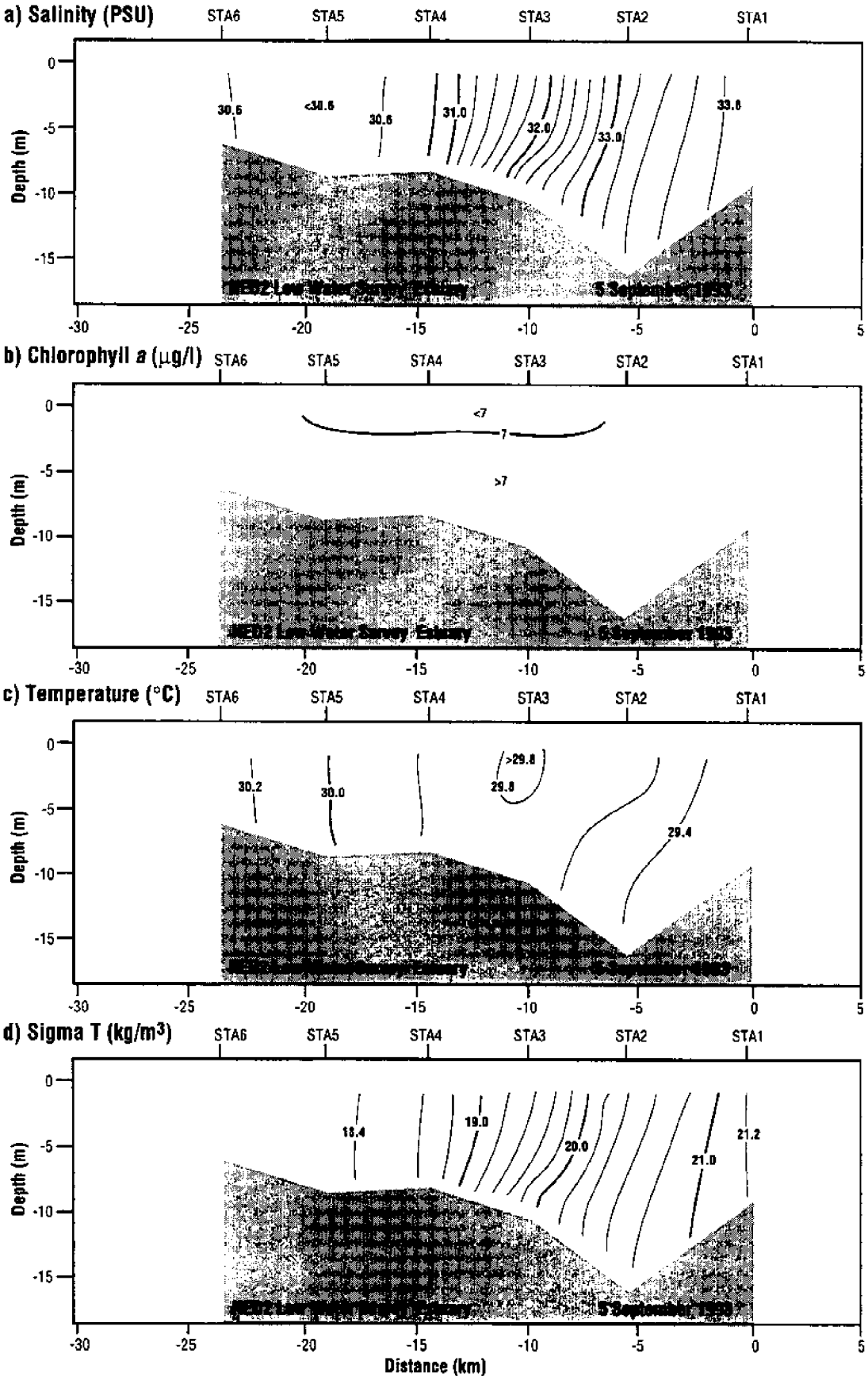

Fig. 22. Estuarine survey in the North Edisto River during low water on 5 September 1993. (a) Salinity; (b) chlorophyll *a*; (c) temperature; (d) σ_t. See Fig.1 for station locations.

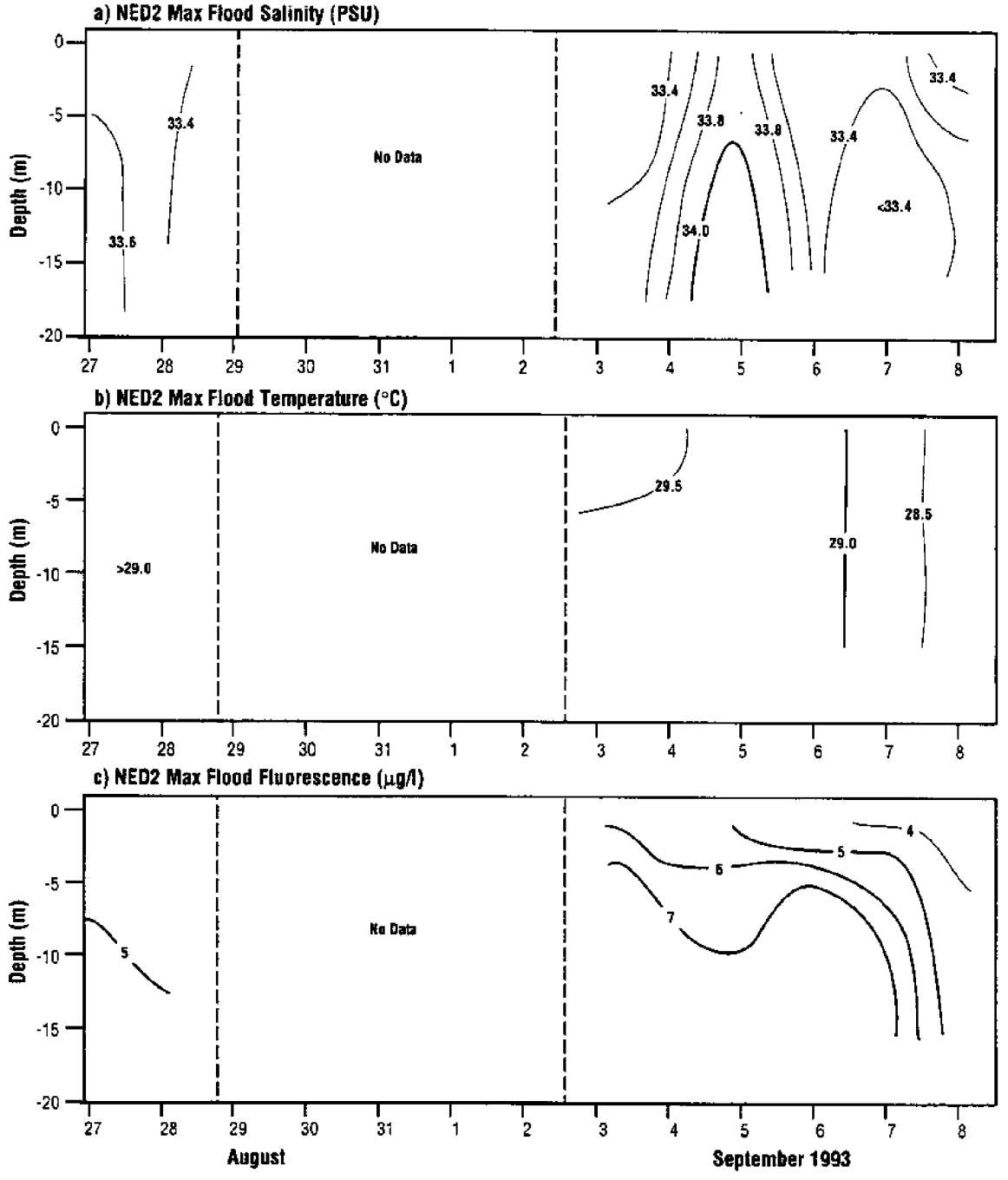

Fig. 23. Time versus depth plots during nightime maximum flood current in the throat of North Edisto Inlet. Only chlorophyll *a* shows a clearly defined trend for NED2. See text for details. (a) Salinity; (b) temperature; (c) chlorophyll *a*.

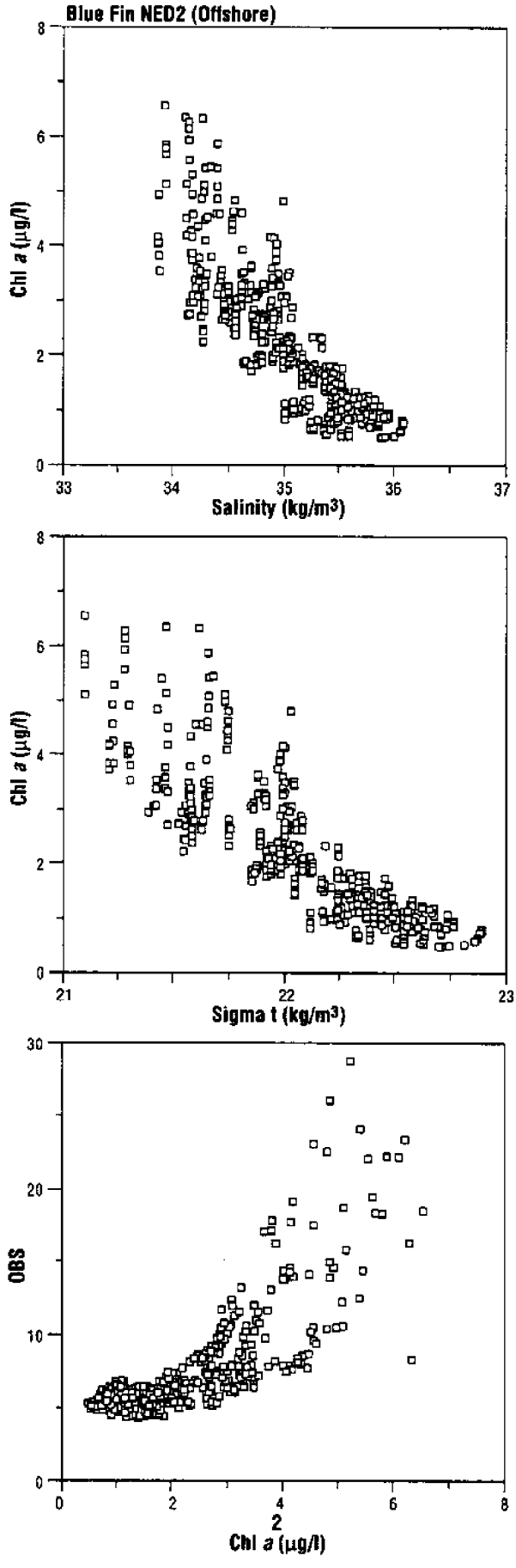

Fig. 24. (a) Chlorophyll *a* versus salinity; and (b) chlorophyll *a* versus σ_t and (c) chlorophyll *a* versus optical backscatter (400 * volts) for all offshore stations.

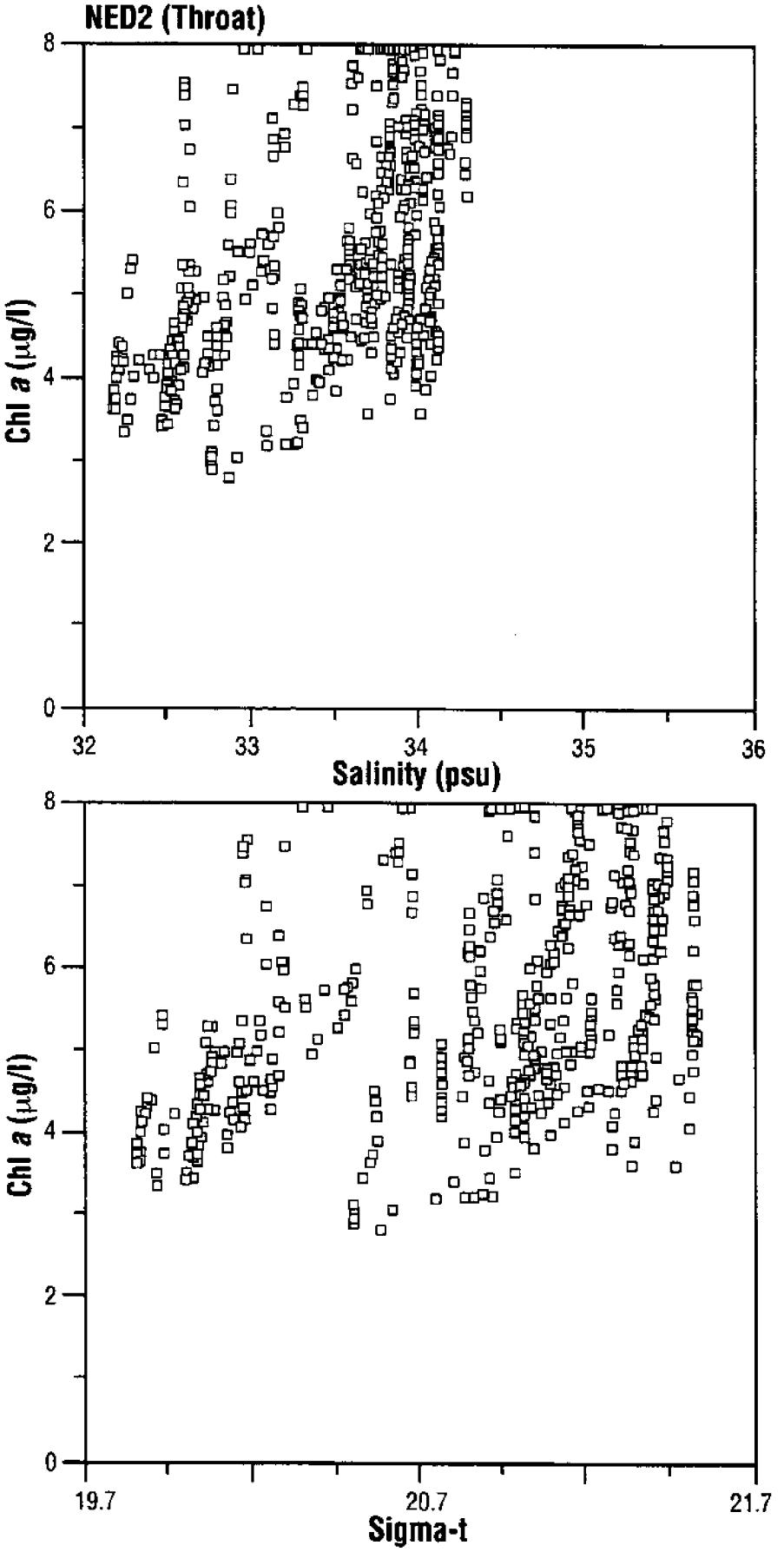

Fig. 25. (a) Chlorophyll *a* versus salinity; and (b) chlorophyll *a* versus σ_t observed in the throat of the inlet.

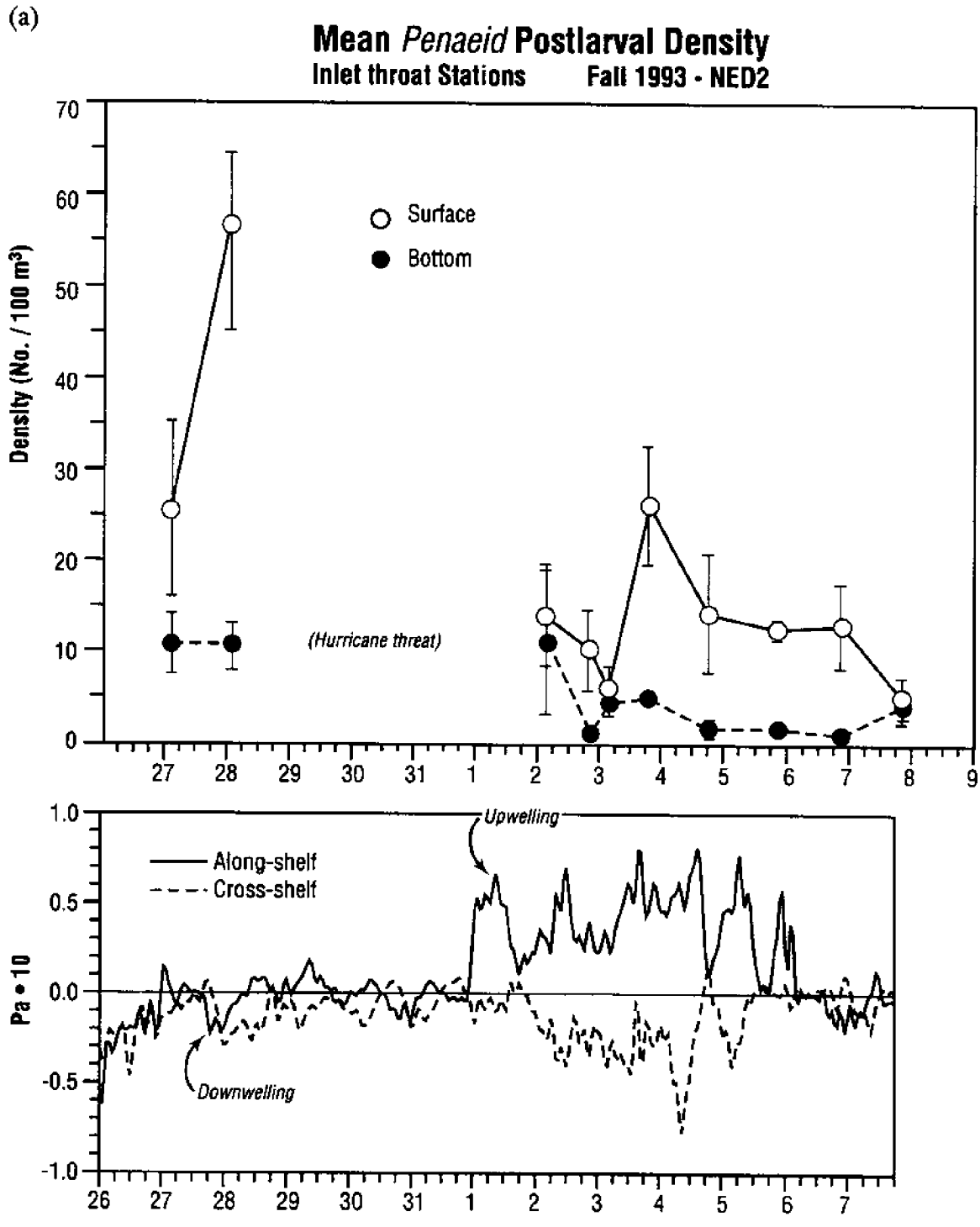

Figure 26. Mean densities and standard errors (No./100m^3) of (a) *Penaeid* postlarva, and (b) blue crab megalopae in the North Edisto Inlet throat during NED2, August-September 1993. Collections were made during each night time flood tide. Wind stress data for the period is provided in the lower panel.

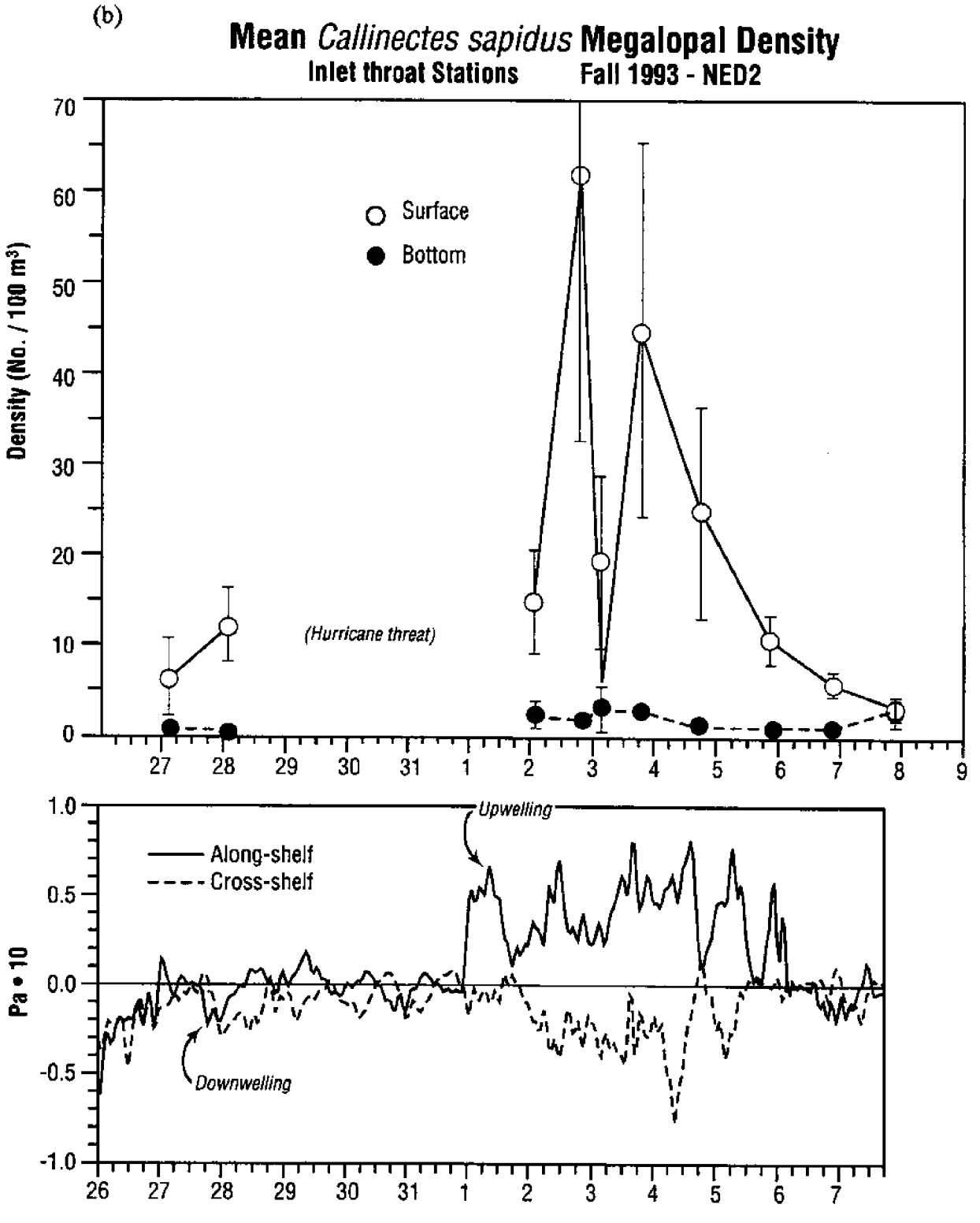

Figure 26. Mean densities and standard errors (No./100m^3) of (a) *Penaeid* postlarva, and (b) blue crab megalopae in the North Edisto Inlet throat during NED2, August-September 1993. Collections were made during each night time flood tide. Wind stress data for the period is provided in the lower panel.

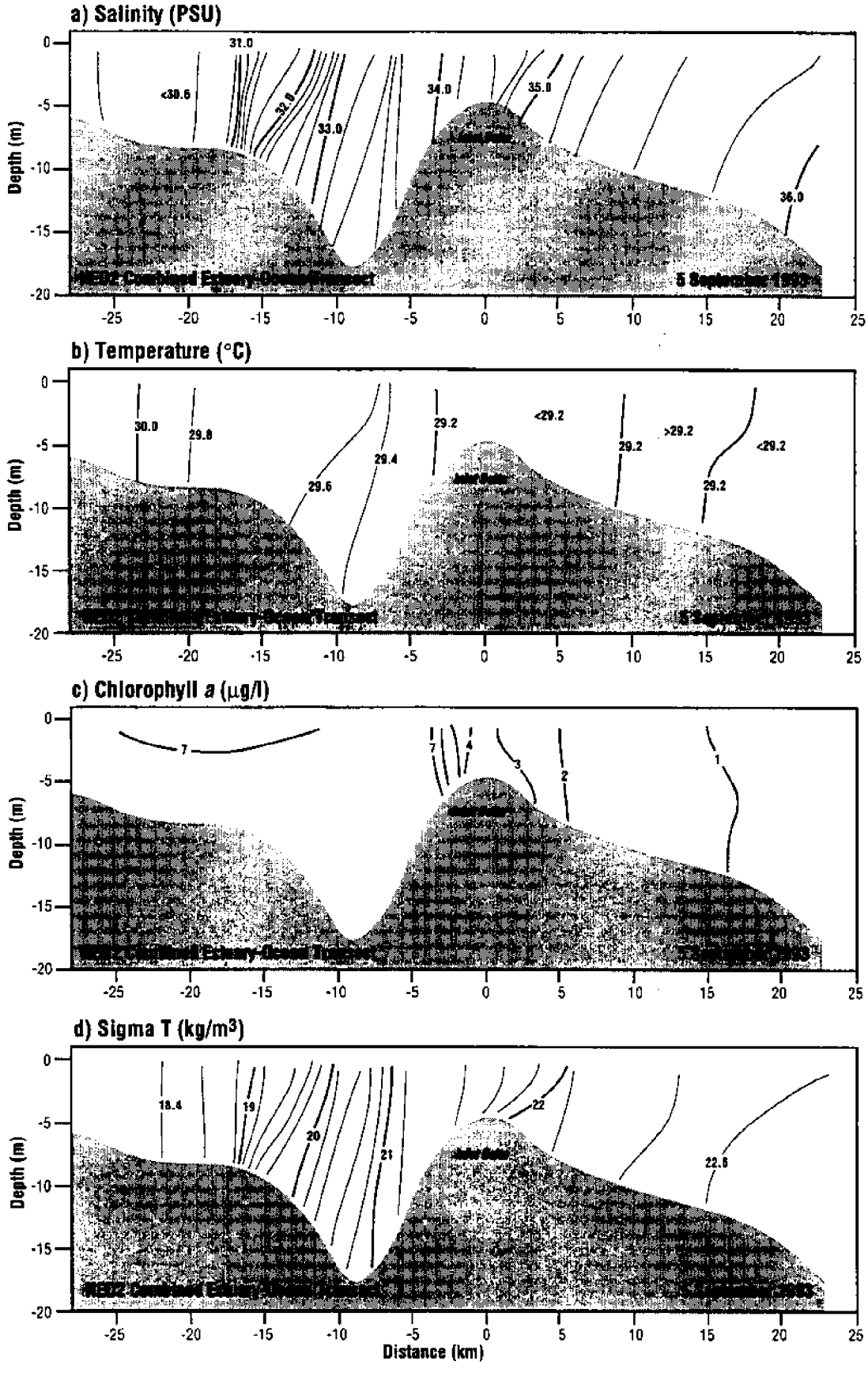

Fig. 27. Combined sections for 5 September of (a) salinity, (b) temperature, (c) chl *a*, (d) and σ_t for OS5 (offshore survey) and the low water estuary survey. Distances originate at Station S0, and distances greater than 0 are on the continental shelf.

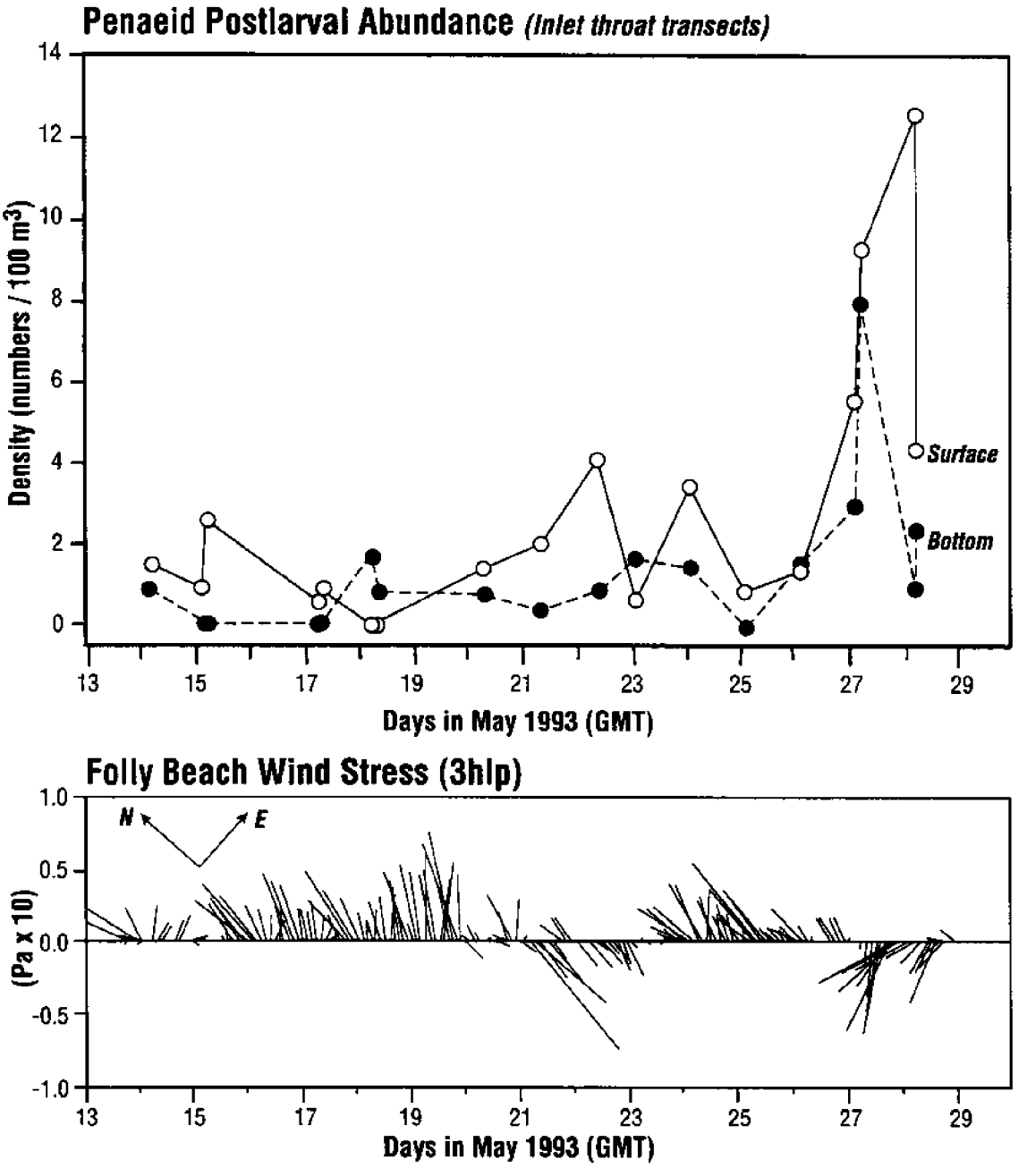

Fig. 28. Density (No./100 m^3) of postlarval Penaeus from surface and bottom plankton samples during NED1, May 1993 (from Blanton et al., 1994). Collections were made at night during flood tide. Wind stress data for the period is provided in the lower panel.